ChemPubSoc Europe

DOI: 10.1002/cmdc.201200484

Design, Synthesis, in vitro MAO-B Inhibitory Evaluation, and Computational Studies of Some 6-Nitrobenzothiazole-Derived Semicarbazones

Rati K. P. Tripathi, Omprakash Goshain, and Senthil Raja Ayyannan*[a]

Monoamine oxidase B (MAO-B) is an important drug target for the treatment of neurological disorders. A series of 6-nitrobenzothiazole-derived semicarbazones were designed, synthesized, and evaluated as inhibitors of the rat brain MAO-B isoenzyme. Most of the compounds were found to be potent inhibitors of MAO-B, with IC_{50} values in the nanomolar to micromolar range. Molecular docking studies were performed with AutoDock 4.2 to deduce the affinity and binding mode of these inhibitors toward the MAO-B active site. The free energies of binding (ΔG) and inhibition constants (K_i) of the docked compounds were calculated by the Lamarckian genetic algorithm (LGA) of AutoDock 4.2. Good correlations between the calculated and experimental results were obtained. 1-[(4-Chlorophenyl)-(phenyl)methylene]-4-(6-nitrobenzothiazol-2-yl)semicarbazide emerged as the lead MAO-B inhibitor, with top ranking in both the experimental MAO-B assay (IC_{50}: 0.004 ± 0.001 μM) and in computational docking studies (K_i: 1.08 μM). Binding mode analysis of potent inhibitors suggests that these compounds are well accommodated by the MAO-B active site through stable hydrophobic and hydrogen bonding interactions. Interestingly, the 6-nitrobenzothiazole moiety is stabilized in the substrate cavity with the aryl or diaryl residues extending up into the entrance cavity of the active site. According to our results, docking experiments could be an interesting approach for predicting the activity and binding interactions of this class of semicarbazones against MAO-B. Thus, a binding site model consisting of three essential pharmacophoric features is proposed, and this can be used for the design of future MAO-B inhibitors.

Introduction

Monoamine oxidases (MAOs; amine–oxygen oxidoreductase; EC 1.4.3.4) contain the flavin adenine dinucleotide (FAD) cofactor covalently bonded to a cysteine residue,[1] and are involved in catalyzing the oxidative deamination of monoamine neurotransmitters, resulting in the modulation of their concentrations in brain and peripheral tissues.[2,3] In mammals, MAOs are present in two isoenzyme forms, namely MAO-A and MAO-B, which are located predominantly in the outer mitochondrial membrane of neuronal, glial, and other cells.[4] Physiologically, MAOs cause oxidation of biogenic neurotransmitters such as dopamine, norepinephrine, 5-hydroxytryptamine (5-HT, serotonin), and β-phenethylamine, as well as xenobiotic amines such as tyramine and benzylamine.[5,6] MAO-A has greater affinity for serotonin and norepinephrine and is more sensitive to inhibitors like clorgyline and moclobemide. On the other hand, MAO-B is selectively inhibited by low concentrations of selegiline (L-deprenyl) and rasagiline.[7,8]

MAO-mediated oxidations lead to the formation of aldehyde as the main product along with several neurotoxic chemical species such as hydrogen peroxide and ammonia as byproducts. Given the formation of these neurotoxic byproducts, prolonged or excessive activity of these enzymes may be responsible for mitochondrial damage and neurodegenerative disturbances. Therefore, the development of MAO inhibitors (MAOIs) represents a very important and useful approach for the treatment of various neurological and neuropsychiatric disorders.[9,10] Nonselective or irreversible inhibitors have shown various drawbacks such as cumulative effects and the so-called "cheese effect", whereby the catabolism of ingested amines is blocked; these have rendered the therapeutic use of nonselective MAOIs obsolete. MAO-A-selective inhibitors are used for the treatment of mental disorders, and have found use as antidepressants and anxiolytics,[11–16] whereas MAO-B-selective inhibitors are used as adjuncts for the treatment of Parkinson's, Alzheimer's, and Huntington's diseases.[17–23]

The determination of the crystal structure of MAO-B by Binda and colleagues has resolved the catalytic mechanism involved in the selective interactions between the enzymes and their ligands or substrates, and has provided a better understanding of the pharmacophoric requirements for the rational design of potent and selective inhibitors with therapeutic potential.[24] The RCSB Protein Data Bank (PDB) availability of experimentally determined co-crystals of MAO-B with various inhibitors has allowed researchers to also perform computational studies with the aim of proposing preferred binding modes, thereby aiding in the rational design of new MAO-B inhibitors.

There have been reports on the influence of hydrophobicity at the active site on the affinity of various types of MAO inhibitors or substrates.[25,26] A wide variety of structurally unrelated

[a] R. K. P. Tripathi, O. Goshain, S. R. Ayyannan
21, Pharmaceutical Chemistry Research Laboratory
Department of Pharmaceutics, Indian Institute of Technology
Banaras Hindu University, Varanasi 221005, Uttar Pradesh (India)
E-mail: asraja.phe@itbhu.ac.in

selective inhibitors of MAO containing a basic nitrogen atom held in a relatively rigid environment, e.g., as part of a heterocycle, are well known.[27–29] A diverse class of MAO-B inhibitors including aryl hydrazines[30–32] and their heterocyclic analogues[33,34] bearing thiazole and pyrazole rings have been studied, and their specific mechanism of action has been fully investigated. Several aryl hydrazones and semicarbazones possessing lipophilic substituents such as a benzyloxy group were found to possess activity against MAO-B with IC_{50} values in the range of 10^{-8} to $>10^{-5}$ M.[35] The structures of some heterocyclic MAO-B inhibitors and aryl hydrazones and semicarbazones are shown in Figure 1 (compounds **1**–**6**).[36–39]

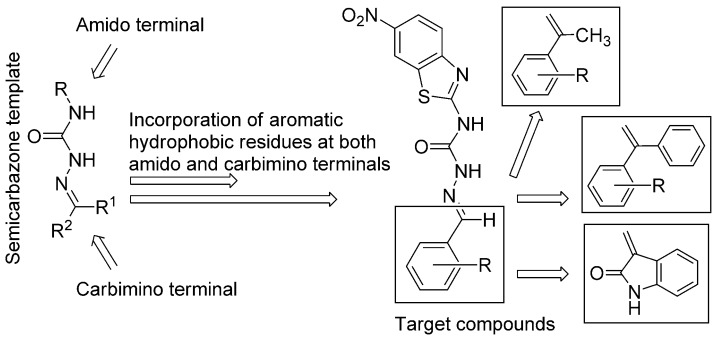

Figure 2. Design of heterocyclic semicarbazones bearing 6-nitrobenzothiazole and isatin moieties.

The extraction of pharmacophore features of known potent MAO-B inhibitors has revealed the importance of two elements: namely hydrophobic and hydrogen bonding (acceptor and donor) sites in their structures. Further in silico modeling studies of known MAO-B inhibitors against MAO-B have suggested that these compounds occupy both the substrate and entrance cavities, and a majority of them are stabilized through hydrophobic and hydrogen bonding interactions with the complementary residues in the active site.[40]

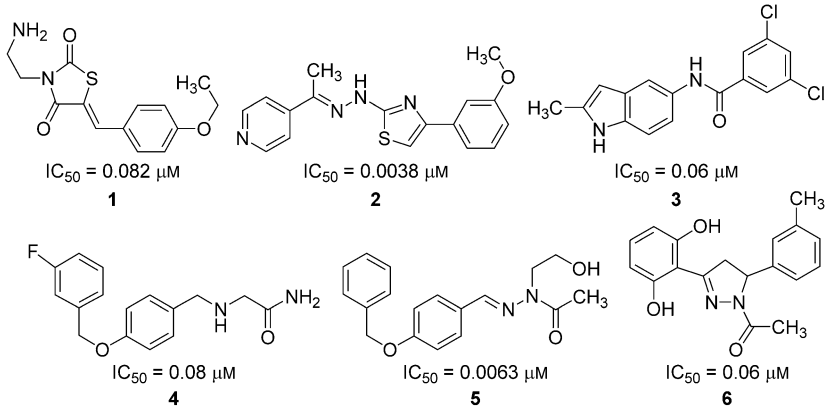

Figure 1. Structures of some heterocycles, hydrazones, and semicarbazones possessing potent MAO-B inhibitory properties.

Semicarbazones[41,42] possessing a R-NH-(C=O)-NH-N=C-R^1R^2 moiety have been well documented as novel scaffolds for the development of new therapeutic agents for the treatment of CNS disorders. Both isatin-[41a] and benzothiazole-derived[42] semicarbazones have been reported to possess potential anticonvulsant and antidepressant activities with no or minimal neurotoxicity. On the other hand, isatin (indol-2,3-dione), an endogenous compound, was found to possess both MAO-A and MAO-B inhibitory properties with no neurotoxicity.[43] With a view to identify novel heterocyclic compounds as potent MAO-B inhibitors that could serve as potential lead molecules for drug discovery, we designed a series of heteroaryl semicarbazones by incorporating 6-nitrobenzothiazole and arylidene, diarylmethylene, and isatin residues at amido and carbimino termini in the semicarbazone scaffold. The design approach is depicted in Figure 2. As a stable electron-rich region, the versatile semicarbazone moiety can serve as a hydrogen bonding site, whereas the substituted aryl systems at the amido and carbimino termini can offer hydrophobic interactions to the active site of MAO-B. The work presented herein includes the synthesis, in vitro MAO-B inhibition, and computational studies of 6-nitrobenzothiazole-derived semicarbazones **10**–**34** along with a comparison of their MAO-B binding and inhibitory potential against those of the reference drugs.

Computational analysis of MAO-B inhibitors by the docking simulation software AutoDock 4.2 was performed to gain structural insight into the binding modes and possible interactions of the inhibitor compounds with the active site of human recombinant MAO-B and to determine the binding orientation, free energy of binding (ΔG), and inhibition constants (K_i) of the experimentally tested MAO-B inhibitors.

Results and Discussion

Chemistry

(6-Nitro-1,3-benzothiazol-2-yl)semicarbazones **10**–**30** were synthesized by the method outlined in Scheme 1 from 1-(6-nitro-1,3-benzothiazol-2-yl)semicarbazide (**9**).[42] The intermediate 1-(6-nitro-1,3-benzothiazol-2-yl)urea (**8**) was prepared by treating 2-amino-6-nitrobenzothiazole (**7**) with aqueous sodium cyanate in the presence of glacial acetic acid; compound **9** was obtained by treating 1-(6-nitro-1,3-benzothiazol-2-yl)urea (**18**) with hydrazine hydrate at reflux. The final products **10**–**34** were obtained in good yields by condensation of compound **9** with the appropriate aldehydes or ketones.

Isatin-substituted semicarbazones **31**–**34** were synthesized by the conventional condensation reaction between compound **9** and 5-(un)substituted isatin in ethanol (Scheme 2).[42]

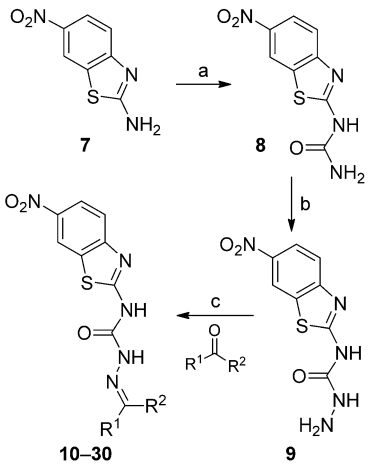

Scheme 1. Synthesis of compounds **10**–**30**. *Reagents and conditions:* a) Glacial AcOH/NaOCN, RT, 3 h; b) EtOH, $NH_2NH_2{\cdot}H_2O$, reflux, 6–7 h; c) EtOH, reflux, glacial AcOH, 30–52 h.

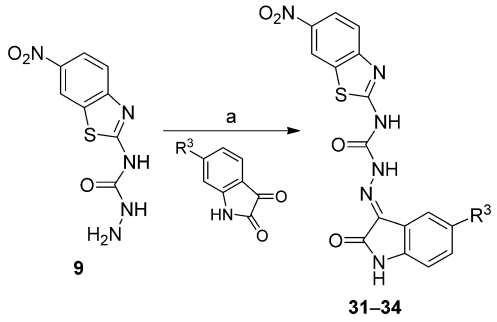

Scheme 2. Synthesis of compounds **31**–**34**. *Reagents and conditions:* a) EtOH, glacial AcOH, reflux, 10–30 h.

Analytical and spectral data for all synthesized compounds are in good agreement with their composition. Physicochemical characteristic data for all final compounds **10**–**34**, along with their MAO-B IC_{50} values, are listed in Table 1.

In vitro MAO-B inhibition studies

Table 1 lists the in vitro rat brain MAO-B inhibitory activity of final compounds **10**–**34** as well as the reference compounds selegiline, safinamide, and isatin. The inhibition data are expressed as IC_{50} values. All the synthesized compounds **10**–**34** showed MAO-B inhibition in the micromolar to nanomolar range; IC_{50} values toward MAO-B range from 0.004 ± 0.001 μM for compound **28** to 2.154 ± 0.095 μM for compound **31**. Indeed, structural modifications attempted in all compounds of the series generally resulted in improved activity. In particular, enhancement of lipophilicity by incorporating monoaryl or diaryl rings or an isatin residue at the carbimino terminus of semicarbazone resulted in increased inhibitory activity against MAO-B.

Compound **28** (1-[(4-chlorophenyl)(phenyl)methylene]-4-(6-nitrobenzothiazol-2-yl)semicarbazide, $IC_{50} = 0.004 \pm 0.001$ μM) emerged as the most active MAO-B inhibitor in the study, followed by **25** (1-[1-(4-fluorophenyl)ethylidene]-4-(6-nitrobenzothiazol-2-yl)semicarbazide, $IC_{50} = 0.017 \pm 0.005$ μM) and **27** (1-(diphenylmethylene)-4-(6-nitrobenzothiazol-2-yl)semicarbazide, $IC_{50} = 0.018 \pm 0.002$ μM). All three inhibitors were found to be more potent than selegiline.

In general, improvement in MAO-B inhibitory activity was observed by substituting the H atom with a methyl group at R^2 (compare **23**–**25**, **27**, **28**, and **10**–**22**). Particularly compound **28** ($IC_{50} = 0.004 \pm 0.001$ μM) was found to be nearly fivefold more potent than selegiline ($IC_{50} = 0.020 \pm 0.008$ μM). An increase in the methoxy substitutions on the phenyl ring (at the carbimino terminus) caused a decrease in activity toward MAO-B (compare **15**, **20**, **21**, and **22** with **23**–**25**, **27**, and **28**). In contrast, introduction of a fluoro or chloro group at the *para* position of the phenyl ring at R^1 along with the methyl group at R^2 (**25** and **28**) increased potency. Thus, substitution of fluoro, bromo, and chloro groups on the distal phenyl ring, preferably at the *para* position, enhanced MAO-B inhibitory activity, whereas the presence of bulkier substituents such as methoxy or nitro groups caused decreased activity.

Among the isatin-3-substituted semicarbazones **31**–**34**, 5-nitroisatin derivative **34** showed the most potent MAO-B inhibition followed by bromo- and chloro-substituted derivatives **32** and **33**, respectively. The unsubstituted derivative **30** was found to be least active. A more detailed discussion on the SAR of these inhibitors is included along with their computational binding and experimental activity data in the next section. The synthesized compounds were also assayed for their in vitro MAO-A inhibitory activity, and the data (unpublished results) revealed that some of the compounds (namely, **18**, **28**, **27**, and **33**) showed good selectivity (56- to 102-fold) toward the MAO-B isoenzyme.

Computational studies

In silico docking studies were carried out to evaluate the affinity and binding interactions of experimentally tested 6-nitrobenzothiazole-derived semicarbazones **10**–**34** against human recombinant MAO-B. The structural and binding mode analyses of compounds **10**–**34** with MAO-B were carried out under an automated molecular docking simulation by AutoDock 4.2. The best-scoring molecules from the largest cluster were considered for further structural and interaction studies. The theoretical K_i values and free energies of binding are listed in Table 2.

To validate the docking protocol, the AutoDock-generated docked pose of the reference inhibitor safinamide (2-[({4-[(3-fluorophenyl)methoxy]phenyl}methyl)amino]propanamide) into the MAO-B active site was compared with the orientation of co-crystallized safinamide (gold standard pose, GSP) MAO-B complex (PDB ID: 2V5Z) (Figure 3a). The docked safinamide shared a similar orientation and binding mode as those of the co-crystallized safinamide. The binding orientation of safinamide in MAO-B traverses both entrance and substrate cavities. The nonpolar 3-fluorobenzyloxy moiety is located in the entrance cavity space surrounded by residues Pro 102, Leu 164, Phe 168, Ile 198, Ile 199, Trp 199, Ile 316, and Tyr 326, whereas

Table 1. Physicochemical characteristics and MAO-B inhibitory data for compounds **10**–**34**.

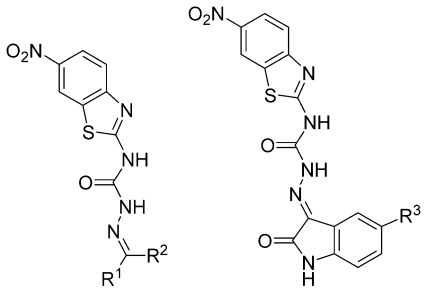

10–30 **31–34**

Compd	R^1	R^2	R^3	Yield [%]	R_f[a]	IC_{50} [μM][b]
10	CH_3	CH_3	–	75.20	0.75	0.132 ± 0.027
11	C_6H_5	H	–	56.67	0.74	0.069 ± 0.006
12	4-Br C_6H_4	H	–	58.67	0.71	0.095 ± 0.067
13	4-OH C_6H_4	H	–	49.02	0.68	0.133 ± 0.016
14	4-NO_2 C_6H_4	H	–	49.85	0.66	0.299 ± 0.051
15	4-OCH_3 C_6H_4	H	–	54.87	0.72	0.286 ± 0.081
16	4-$N(CH_3)_2$ C_6H_4	H	–	78.89	0.71	0.064 ± 0.001
17	2,3-Cl_2 C_6H_3	H	–	64.94	0.69	0.406 ± 0.023
18	2,6-Cl_2 C_6H_3	H	–	68.36	0.72	0.063 ± 0.018
19	2,4-Cl_2 C_6H_3	H	–	56.19	0.73	0.126 ± 0.009
20	3,4-$(OCH_3)_2$ C_6H_3	H	–	69.90	0.73	0.091 ± 0.004
21	2,5-$(OCH_3)_2$ C_6H_3	H	–	63.56	0.67	0.757 ± 0.052
22	3,4,5-$(OCH_3)_3$ C_6H_2	H	–	68.78	0.70	0.836 ± 0.192
23	C_6H_5	CH_3	–	62.97	0.71	0.022 ± 0.004
24	4-Br C_6H_4	CH_3	–	57.25	0.69	0.054 ± 0.003
25	4-F C_6H_4	CH_3	–	65.43	0.63	0.017 ± 0.005
26	4-OH C_6H_4	CH_3	–	58.78	0.76	1.070 ± 0.647
27	C_6H_5	C_6H_5	–	53.45	0.71	0.018 ± 0.002
28	4-Cl C_6H_4	C_6H_5	–	62.56	0.66	0.004 ± 0.001
29	4-OH C_6H_4	C_6H_5	–	76.45	0.77	0.114 ± 0.035
30	4-Cl C_6H_4	4-Cl C_6H_4	–	73.34	0.74	0.512 ± 0.002
31	–	–	H	72.59	0.61	2.154 ± 0.095
32	–	–	Br	75.92	0.72	0.055 ± 0.010
33	–	–	Cl	76.22	0.70	0.188 ± 0.024
34	–	–	NO_2	74.34	0.65	0.029 ± 0.007
selegiline	–	–	–	–	–	0.020 ± 0.008
safinamide[48a]	–	–	–	–	–	0.100
isatin[43]	–	–	–	–	–	3.00

[a] Solvent system: CH_3Cl/CH_3OH/toluene 5:4:1. [b] Values represent the assay drug concentration that give 50% inhibition of MAO-B activity, and are the mean ± SEM; statistical significance: $p < 0.05$ versus the corresponding IC_{50} values obtained against MAO-B, as determined by ANOVA/Dunnett's test.

the polar propanamidyl moiety occupies the substrate cavity embedded around Tyr 60, Cys 172, Tyr 188, Gln 206, Phe 343, Tyr 398, and Tyr 435.

Visual inspection of computationally docked binding poses of all compounds within the active site of MAO-B resulted in the following observations: All test compounds are well stabilized in both the substrate and entrance cavities of the MAO-B active site. The binding mode of best-scored inhibitors further suggests that the rigid hydrophobic 6-nitrobenzothiazole moiety is caged into the substrate cavity, while the hydrophobic arylidene or diarylmethylene or isatin residue present in the carbimino terminus is stabilized in the entrance cavity. The selective and preferential stabilization of the 6-nitrobenzothiazole moiety may be due to the presence of a polar nitro group, which may be predicted to interact with the water molecules present in the substrate cavity. A few exceptions are found with inhibitors **13** and **34**, possessing polar hydroxy and nitro groups respectively, for which the binding orientation is completely the reverse; eventually these inhibitors showed lower binding affinity than the others.

Poor binding affinity and higher K_i values are observed with inhibitors **13**, **21**, **16**, **20**, **14**, **10**, and **22**, which bear one or more alkoxy, nitro, or hydroxy substituents on the distal aryl rings present at the carbimino terminus of semicarbazones. In contrast, the compounds bearing either a chloro or bromo substituent on the carbimino terminal aryl ring (**12**, **17**, **18**, **28**, and **30**) displayed better binding affinity toward MAO-B. This clearly demonstrates the role of electronegative chloro and bromo substituents, which enhance the stabilization of hydrophobic aryl rings into the complementary regions of the entrance cavity. In addition, the substitution of the H atom at R^2 (compound **13**) with a methyl group (compounds **28**, **27**, and **25**) caused improved binding and inhibitory potency. Compared with the monoaryl-substituted derivatives (at the carbimino terminus), the diaryl derivatives showed better binding and K_i values, which may be due to the additional hydrophobic interactions with the complementary hydrophobic residues of the entrance cavity.

Semicarbazones **31**–**34** possessing both benzothiazole and isatin residues at amido and carbimino termini, respectively, generally showed a similar binding orientation, but higher affinity toward MAO-B than the mono- or diaryl-substituted compounds. The ranking of these inhibitors according to computational data is **32** > **33** > **31** > **34**, whereas the ranking as per the experimental inhibitory data is **34** > **32** > **33** > **31**. Interestingly, among compounds **31**–**33**, an excellent correlation between virtual and experimental data is observed. Except for the binding mode of **34**, in which the isatin group is stabilized into substrate cavity while the benzothiazole is caged in the entrance cavity, all others (compounds **31**–**33**) shared similar binding modes as those of **11**–**30** except compound **13**. This rather unusual reversed binding mode for **34** may be due to the presence of a 5-nitro substituent, which enhances the po-

Table 2. Free energies of binding and calculated inhibition constants for compounds **10**–**34**, listed in ranking order.

Rank	Compd	ΔG [kcal mol^{-1}]	K_i [μM]
1	**28**	−8.14	1.08
2	**27**	−7.99	1.39
3	**18**	−7.92	1.55
4	**29**	−7.73	2.15
5	**30**	−7.73	2.15
6	**32**	−7.60	2.69
7	**33**	−7.58	2.77
8	**23**	−7.11	6.16
9	**24**	−7.08	6.43
10	**26**	−7.01	7.32
11	**31**	−6.93	8.39
12	**19**	−6.92	8.47
13	**34**	−6.79	10.51
14	**12**	−6.78	10.8
15	**15**	−6.75	11.24
16	**17**	−6.67	12.94
17	**25**	−6.64	13.6
18	**11**	−6.62	13.94
19	**13**	−6.39	20.79
20	**21**	−6.19	28.89
21	**16**	−6.13	32.07
22	**20**	−6.04	37.69
23	**14**	−5.67	70.36
24	**10**	−5.46	100.27
25	**22**	−5.43	104.38
–	safinamide[a]	−5.93	45.23
–	isatin	−4.74	333.71

[a] $IC_{50} = 100$ nM.[48a]

larity of the hydrophobic isatin residue (even more polar than the 6-nitrobenzothiazole ring), thereby guiding it to the substrate cavity. Furthermore, the binding mode of **34** is found to match that of isatin (PDB ID: 1OJA), and this may be the reason for its greater potency in the experimental MAO-B assay ($IC_{50} = 0.029 \pm 0.007$ μM) than others (compounds **31**–**33**). The superimposed binding modes of **31**–**34** along with the reference GSP of isatin are shown in Figure 3b.

Important is the observation that the 6-nitro group present on the benzothiazole moiety may be involved in interactions—possibly hydrogen bonding—with the fluxional water molecules present in the large substrate cavity of the MAO-B active site. This interaction may be responsible for the preferential and selective orientation of 6-nitrobenzothiazole (for **10**–**33**) and 5-nitroisatin (for **34**) moieties into the substrate cavity.

Further investigation of the interactions of all inhibitors **10**–**34** with the anchoring amino acid residues present in the active site of MAO-B led to the following observations: The potential binding sites of these inhibitors were found to be occupied in the wide active site cavity surrounded by residues Ser59, Tyr60, Phe168, Leu171, Cys172, Tyr188, Ile199, Gln206, Lys296, Tyr326, Tyr398, and Tyr435; this is very similar to the binding sites of the standard inhibitor safinamide. This proves that the effective binding sites are present in the 6-nitrobenzothiazole-derived semicarbazones, and that these compounds possess the potential to inhibit MAO-B. Furthermore, these inhibitors are stabilized by π–π stacking and hydrogen bonding interactions.

All compounds showed π–π interactions; a π–π interaction with the Tyr398 residue are observed for compounds **10**, **12**–**14**, **16**–**21**, **24**–**28**, **31**–**33**, and **34**, and with Tyr435 for compounds **11**, **13**, **15**, **17**, **18**, **20**, **22**, **23**, **25**–**30**, **33**, and **34**. Moreover, **15** and **22** were found to undergo π–π interactions with Tyr326. Moreover, compounds **12** and **18** are stabilized by π–σ and π–cation interactions, respectively. A π–σ interaction with FAD was observed for compounds **19**–**24**, **26**, **29**, and **32**. Thus, in most of the potent compounds, preferably π–π hydrophobic and hydrogen bonding interactions were observed to be responsible for mediating biological activity. A graphical inspection was made to identify the possible binding orientation and interactions of **10**–**34** within the MAO-B active site. We focused our attention only on the binding modes of the most active compounds **28**, **27**, **18**, and **32**.

Binding mode of 28 and 27

Examination of one of the best-ranked docking solutions of **28** (Figure 3c) and **27** (Figure 3d) revealed that the 6-nitrobenzothiazole nucleus is located in the substrate cavity, while the carbimino side chain is extended toward the entrance cavity of MAO-B. Furthermore, the diarylidene-bearing carbimino side chain of **28** occupies the entrance hydrophobic cleft formed by Pro102, Pro104, Trp119, Leu164, Ile198, Ile199, Thr201, Ile316, and Tyr326, whereas the benzothiazole moiety in the substrate cavity is embedded in a large hydrophobic cage formed by residues Ser59, Tyr60, Cys172, Gln206, Tyr398, and Tyr435. The benzene and thiazole rings of the benzothiazole nucleus are involved in a π–π interaction, with Tyr398 at interplane distances of ~3.81 and ~4.99 Å, respectively. In addition, a π–π interaction was also observed between Tyr435 and the benzene ring of benzothiazole, with a distance of ~5.24 Å. Importantly, the chlorine atom of **28** is stabilized by hydrogen bond interaction with the hydroxy group of Thr201 (d = 2.49 Å) located in the entrance cavity. Because the addition of chlorine would enhance the lipophilicity of a phenyl ring, these interactions may explain the observation that chlorine substitution of the phenyl side chain of **28** enhances MAO-B inhibitory potency. Besides this, electrostatic interactions with Leu164 and Tyr326 were also evident (Figure 3c).

Conversely, the benzene moiety of **27** (Figure 3d) is possibly stabilized by π–π interactions with Tyr398 at an interplane distance of ~4.82 Å. Varying degrees of electrostatic and van der Waals interactions with residues Trp119, Leu164, Ile198, Cys172, Ile199, Gln206, and Ile316 may further contribute to the binding and stabilization of **37** in the cavity space. In addition, a hydrogen bond interaction with the oxygen atom of Ile198 at an interplane distance of 2.49 Å is observed.

Binding mode of 18

Visual inspection of the pose of **18** in the MAO-B binding site revealed that the binding orientation is similar to that of the above compounds. That is, the benzothiazole nucleus binds

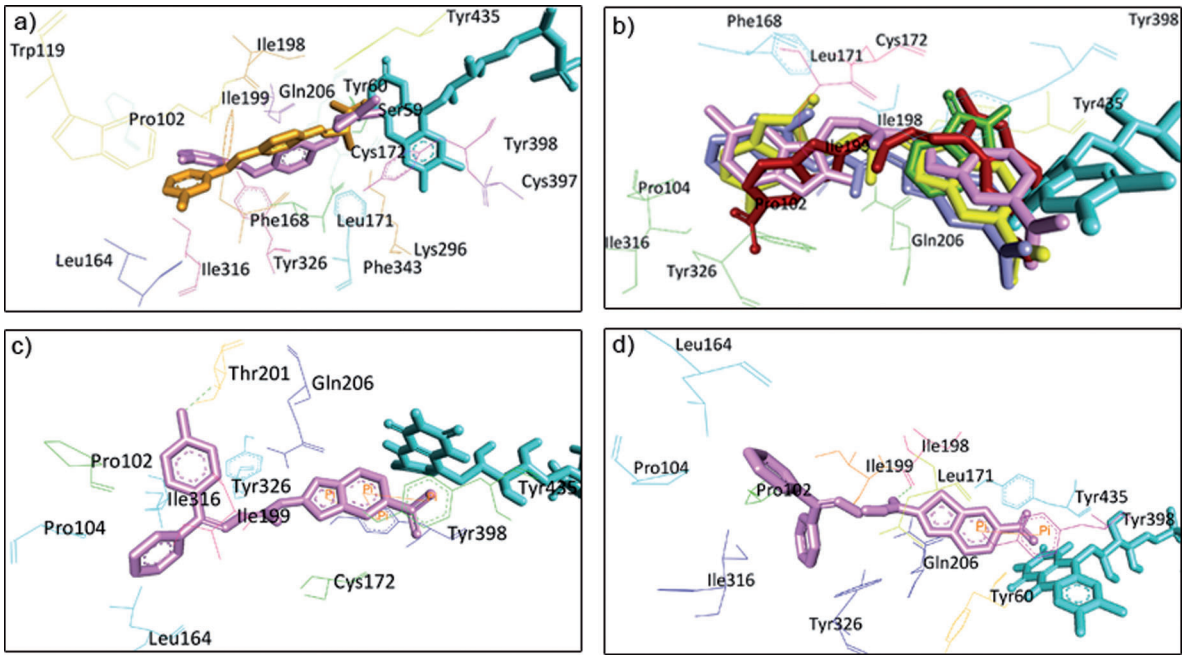

Figure 3. a) AutoDock-generated pose of safinamide (pink) with the GSP of safinamide (brown) (PDB ID: 2V5Z) in the MAO-B active site. b) Superimposed binding modes of isatin-substituted MAO-B inhibitors **31** (violet), **32** (pink), **33** (yellow), and **34** (maroon) along with the GSP of isatin (green). c) Binding interactions of **28** (pink) in the MAO-B active site. d) Binding interactions of **27** (pink) in the MAO-B active site. Selected residues are labeled and displayed in wireframe, and the FAD cofactor is shown as blue sticks in each case.

within the substrate cavity space and is surrounded by residues Ser 59, Tyr 60, Cys 172, Gln 206, Tyr 398, and Tyr 435, whereas the arylidene-bearing carbimino side chain occupies the entrance cavity and is lined by residues Pro 104, Trp 119, Leu 164, Phe 168, Ile 198, Ile 199, Ile 316, and Tyr 326. The benzothiazole system is sandwiched between the aromatic residue Tyr 435, forming π–π stacking interactions. The amino nitrogen atom of the semicarbazone linker is stabilized by hydrogen bond interactions with the oxygen atom of Ile 198 (Figure 4 a). In addition, a π–cation interaction was observed between Tyr 326 and the carbimino nitrogen atom, with an interplane distance of ~2.47 Å.

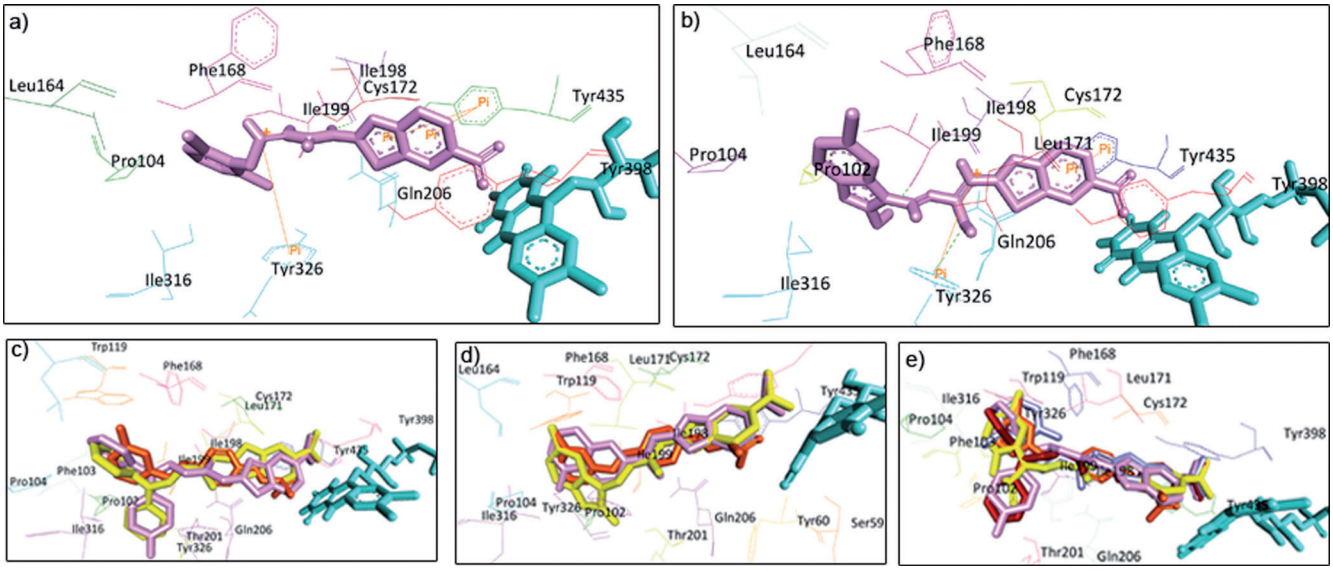

Figure 4. a) Binding interactions of **18** (pink) in the MAO-B active site. b) Binding interactions of **32** (pink) in the MAO-B active site. c) Superimposed binding modes of **28** (pink) and **27** (yellow) with the GSP of safinamide (orange) (PDB ID: 2V5Z) in the MAO-B active site. d) Superimposed binding modes of **18** (pink) and **32** (yellow) with the GSP of safinamide (orange) in the MAO-B active site. e) Superimposed binding modes of the most active MAO-B inhibitors **28** (pink), **27** (maroon), **18** (violet), and **32** (yellow) along with the GSP of safinamide (orange) in the MAO-B active site. Selected residues are labeled and displayed in wireframe, and the FAD cofactor is shown as blue sticks in each case.

Binding mode of 32

Analysis of the most active benzothiazole- and isatin-derived inhibitor **32** in complex with MAO-B revealed that the benzothiazole ring is oriented in the substrate cavity, whereas the carbimino side chain bearing the isatin residue is directed toward the entrance cavity (Figure 4b). This orientation contradicts that of the most active inhibitor **34** of same class. The isatin moiety stabilized in the entrance cavity is surrounded by residues Trp119, Pro104, Leu164, Phe168, Ile198, Ile199, Ile316, and Tyr326. The benzothiazole ring is inserted into the substrate cavity, forming an aromatic cage framed by Ser59, Tyr60, Gln206, Tyr398, and Tyr435, and the binding is further stabilized by π–π interactions between Tyr435 and the benzene ring at an interplane distance of ~4.85 Å. Moreover, two hydrogen bonds are also observed for the carbonyl oxygen atom of the isatin moiety and the carbonyl oxygen of Ile199, and between the carbonyl oxygen of the carbimino side chain and the hydroxy group of Tyr326. In addition, a π–cation interaction between the amino nitrogen atom of the side chain and Tyr326 is also observed, with an interplane distance of 5.36 Å. It is observed that the bromine atom of **32** undergoes significant van der Waals interactions with Leu164, Phe168, and Ile316. However, the lower affinity of **32** relative to **28**, **27**, and **18** may be due to the steric bulk imparted by the large hydrophobic isatin moiety. (Figure 4b).

Thus, in this study we have tried to establish how these compounds interact differently in the MAO-B binding pocket. Docking of **27** showed that its stability is due to π–π interactions, van der Waals, and electrostatic forces, whereas the stability of **28**, **18**, and **22** also includes hydrogen bonding interactions along with the above interactions. Primarily to check the congruence of the observed results with the predicted results in terms of binding modes to the MAO-B receptor, superimposition of **28** and **27** (Figure 4c) and **18** and **32** (Figure 4d) was carried out separately and altogether (Figure 4e) with the GSP of safinamide within the MAO-B active site. Good agreement was observed in both cases, as evidenced from the structural screenshots.

The difference in the experimental and theoretical results is due to the difference in the sources of MAO-B enzymes. Hence, we did not expect to obtain exact experimental values by computational calculations. This difference may also arise in the approximations and simplifications made during the computation process; for example, no explicit water molecules were considered during docking simulation. Furthermore, AutoDock 4.2 uses empirical scoring functions for free energy calculations. Considering all these factors, a very reasonable prediction of IC_{50} values, inhibition constants (K_i values), and binding energy was obtained.

Conclusions

In this study, a series of 6-nitrobenzothiazole-based semicarbazones **10**–**34** were synthesized and evaluated as inhibitors of MAO-B. Most synthesized semicarbazones were found to exhibit inhibitory potencies in the micromolar to nanomolar range. Computational docking studies with AutoDock 4.2 were carried out for the first time on semicarbazone-based MAO-B inhibitors against MAO-B. The comparative binding mode analysis of potent MAO-B inhibitors suggests that the optimal binding to the large hydrophobic pocket of the substrate cavity requires a large, rigid heterocyclic ring substituted with a polar nitro group. This polar nitro group may guide and stabilize the benzothiazole ring to the substrate cavity, possibly through interaction with fluxional water molecules present in this cavity. On the other hand, the entrance cavity requires chloro- or bromo-substituted mono or diaryl rings for effective binding and stabilization. Both chloro and bromo substituents on the aryl ring at the carbimino terminus of the semicarbazones enhanced MAO-B inhibitory potencies. Thus, the design approach used on the semicarbazone scaffold produced potent MAO-B inhibitors. Compound **28** (1-[(4-chlorophenyl)-(phenyl)methylene]-4-(6-nitrobenzothiazol-2-yl)semicarbazide) emerged as the lead MAO-B inhibitor, which ranked at the top in both experimental MAO-B assays (IC_{50}: 0.004 ± 0.001 μM) and computational docking studies (K_i: 1.08 μM). The potential binding of this lead inhibitor may be attributed to the presence of a large hydrophobic aryl binding site in the form of 6-nitrobenzothiazole and a diaryl binding sites at the amido and carbimino termini, respectively.

By the analysis of experimental and computational data, the following significant pharmacophoric elements influencing the binding affinity and potency of these MAO-B inhibitors are identified: 1) A large hydrophobic heterocyclic ring preferably substituted with a polar nitro group at the amido terminus of semicarbazone is essential for binding with the substrate cavity of the MAO-B active site. 2) Another hydrophobic aryl ring with electronegative substituents such as chloro and bromo groups is crucial for effective binding and stabilization in the entrance cavity space of MAO-B. 3) A flexible linker possessing hydrogen bonding regions is also essential for guiding the optimal orientation of both hydrophobic aryl residues in their respective binding pockets within the active site of MAO-B. Thus, a binding site model consisting of three essential pharmacophoric features is proposed (Figure 5), and this model can be used in the design of future potent MAO-B inhibitors.

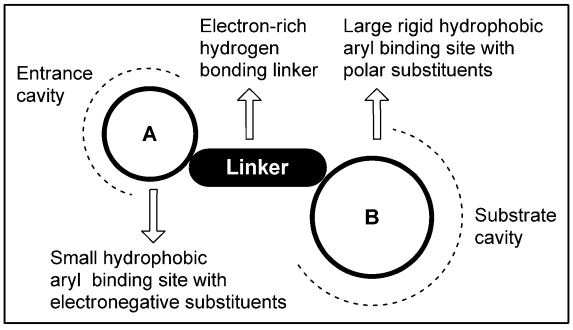

Figure 5. Proposed binding site model for MAO-B inhibitors showing the essential pharmacophoric features.

Experimental Section

Chemistry

All commercial reagents and solvents used were of laboratory grade, obtained from Sigma–Aldrich or Merck. Melting points were determined in open capillary tubes in a Sonar melting point apparatus and are uncorrected. IR and ^{1}H and ^{13}C NMR spectra were recorded in a Shimadzu FT-IR 8400S IR spectrophotometer (KBr) and a JEOL AL300 FT-NMR spectrometer (300 MHz, [D$_6$]DMSO), respectively, at ambient temperature. Chemical shifts (δ) are reported in parts per million (ppm) using tetramethylsilane (TMS) as an internal standard. Signals are designated as follows: s, singlet; d, doublet; t, triplet; m, multiplet. All exchangeable protons were confirmed by the addition of D_2O. FAB MS data were recorded on a JEOL SX 102/Da-600 mass spectrometer/data system using Ar/Xe (6 kV, 10 mA) as the FAB gas. The accelerating voltage was 10 kV, and spectra were recorded at room temperature. Elemental analyses (C, H, and N) were undertaken with a model CE-440 CHN analyzer (Exeter Analytical Inc.). All products had satisfactory C, H and N analyses (within $\pm$0.4%).

Starting materials

2-Amino-6-nitrobenzothiazole **7** (0.03 mol) was dissolved in glacial acetic acid (25 mL) and diluted with distilled H_2O (46–50 mL). To this, a warm solution of NaOCN (0.03 mol, 2.2 equiv) in H_2O (70 mL) was added with vigorous stirring. The mixture was stirred for 3–4 h before being left to stand overnight. The resultant solid was collected by filtration, washed with cold H_2O to remove excess glacial acetic acid, and dried.[43] The yellow-colored crude product 1-(6-nitro-1,3-benzothiazol-2-yl)urea **8** obtained was then recrystallized from 95% EtOH. Thereafter, to a solution of 1-(6-nitrobenzothiazol-2-yl)urea **8** (0.03 mol) in EtOH, $NH_2NH_2{\cdot}H_2O$ (0.03 mol, 2.0 equiv) was added. The content was heated at reflux for 6–7 h and cooled. The crystallized solid yellow-colored product 1-(6-nitro-1,3-benzothiazol-2-yl)semicarbazide **9** formed was filtered, dried, and recrystallized from 95% EtOH. The presence of single spot in TLC denoted completion of reaction.

1-(6-Nitrobenzothiazol-2-yl)urea 8: Yellow solid; mp: 224–226 °C; IR (KBr) $\tilde{\nu}$ = 3514.42 (1° N–H str), 3327.32 (2° N–H str), 3093.92 (aromatic C–H str), 2906.33 (alkane C–H str), 1647.26 (C=O str), 1570.11 (C=N str), 1529.60, 1329.00 (Ar–NO_2 str), 1298.14 cm^{-1} (C–N str); ^{1}H NMR ([D$_6$]DMSO, 300 MHz): δ = 5.88 (s, 1H, N–H), 6.01 (s, 2H, NH_2), 8.48–8.49 (d, 2H, benzothiazole C–H), 9.03 ppm (s, 1H, benzothiazole C–H); ^{13}C NMR ([D$_6$]DMSO, 300 MHz): δ = 117.84 (C7), 120.27 (C5), 122.16 (C4), 126.01 (C7a), 145.64 (C6), 155.81 (C3a), 156.22 (C=O), 174.31 ppm (C2); FAB: *m/z* 238.99 $[M+1]^+$; Anal. for $C_8H_6N_4O_3S$: calcd: C 40.33, H 2.54, N 23.52, found: C 40.35, H 2.53, N 23.51.

1-(6-Nitrobenzothiazol-2-yl)semicarbazide 9: Yellow solid; mp: 258–260 °C; IR (KBr) $\tilde{\nu}$ = 3458.48 (1° N–H str), 3394.53 (2° N–H str), 3091.13 (aromatic C–H str), 2941.54 (alkane C–H str), 1651.12 (C=O str), 1597.11 (C=N str), 1533.46, 1325.14 (Ar–NO_2 str), 1294.28 cm^{-1} (C–N str); ^{1}H NMR ([D$_6$]DMSO, D_2O exchange, 300 MHz): δ = 2.23 (d, 2H, NH_2), 6.08 (s, 1H, CONH), 8.48–8.49 (d, 2H, benzothiazole C–H), 9.07 ppm (s, 1H, benzothiazole C–H); ^{13}C NMR ([D$_6$]DMSO, 300 MHz): δ = 117.50 (C7), 120.37 (C5), 122.83 (C4), 125.56 (C7a), 145.91 (C6), 155.18 (C3a), 154.14 (C=O), 174.62 ppm (C2); FAB: *m/z* 254.24 $[M+1]^+$; Anal. for $C_8H_7N_5O_3S$: calcd: C 37.94, H 2.79, N 27.66, found: C 37.92, H 2.83, N 27.65.

Final products

General procedure for the conventional synthesis of compounds 10–30

The final compounds **10--30** (substituted monoaryl/diaryl semicarbazones) were synthesized by the reaction of 1-(6-nitro-1,3-benzothiazol-2-yl)semicarbazide **9** (0.003 mol) with appropriate aldehydes or ketones (0.003 mol). The reaction mixture was adjusted to pH 5–6 by adding glacial acetic acid and held at reflux for 30–52 h.[43] The solvent was evaporated, and the crude product was purified and recrystallized from 95% EtOH.

4-(6-Nitrobenzothiazol-2-yl)-1-(propan-2-ylidene)semicarbazide (10): Yellow solid; mp: 230 °C; IR (KBr) $\tilde{\nu}$ = 3460.41 (N–H str), 3061.13 (aromatic C–H str), 2947.33 (alkane C–H str), 1654.98 (C=O str), 1570.11 (C=N str), 1535.39, 1329.00 (Ar–NO_2 str), 1301.99 cm^{-1} (C–N str); ^{1}H NMR ([D$_6$]DMSO, D_2O exchange, 300 MHz): δ = 0.90 (s, 6H, CH_3), 6.0 (s, 1H, CONH), 6.99 (s, 1H, =NNH, D_2O exchangeable), 8.48–8.49 (d, 2H, benzothiazole C–H), 9.05 ppm (s, 1H, benzothiazole C–H); ^{13}C NMR ([D$_6$]DMSO, 300 MHz): δ = 16.4 (C″1, CH_3), 22.3 (C′1, CH_3), 117.94 (C7), 120.17 (C5), 122.12 (C4), 126.96 (C7a), 145.81 (C6), 149.68 (C=N), 155.43 (C3a), 157.62 (C=O), 173.91 ppm (C2); FAB: *m/z* 293.24 $[M+1]^+$; Anal. for $C_{11}H_{11}N_5O_3S$: calcd: C 45.04, H 3.76, N 23.88, found: C 45.01, H 3.78, N 23.85.

1-Benzylidene-4-(6-nitrobenzothiazol-2-yl)semicarbazide (11): Yellow solid; mp: 210 °C; IR (KBr): $\tilde{\nu}$ = 3460.41 (N–H str), 3074.66 (aromatic C–H), 1654.12 (C=O), 1570.11 (C=N str), 1531.53, 1329.00 (Ar–NO_2 str), 1294.28 cm^{-1} (C–N str); ^{1}H NMR ([D$_6$]DMSO, D_2O exchange, 300 MHz): δ = 6.02 (s, 1H, CONH), 7.18 (s, 1H, =NNH, D_2O exchangeable), 7.41–7.73 (m, 8H, Ar C–H), 8.19 (s, 1H, C–H), 8.45–8.49 (d, 2H, benzothiazole C–H), 9.15 ppm (s, 1H, benzothiazole C–H); ^{13}C NMR ([D$_6$]DMSO, 300 MHz): δ = 117.80 (C7), 120.13 (C5), 122.64 (C4), 125.43 (C7a), 128.89 (C′3, C′5), 129.25 (C′2, C′6), 131.08 (C′4), 133.92 (C′1), 144.31 (C=N), 145.74 (C6), 155.36 (C3a), 157.21 (C=O), 174.28 ppm (C2); FAB: *m/z* 341.33 $[M+1]^+$; Anal. for $C_{15}H_{11}N_5O_3S$: calcd: C 52.78, H 3.25, N 20.52, found: C 52.75, H 3.27, N 20.50.

1-(4-Bromobenzylidene)-4-(6-nitrobenzothiazol-2-yl)semicarbazide (12): Yellow solid; mp: 237 °C; IR (KBr): $\tilde{\nu}$ = 3510.56 (N–H str), 3091.99 (aromatic C–H str), 1647.26 (C=O str), 1594.88 (C=C str), 1570.11 (C=N str), 1527.67, 1327.07 (Ar–NO_2 str), 1296.21 (C–N str), 553.59 cm^{-1} (C–Br str); ^{1}H NMR ([D$_6$]DMSO, D_2O exchange, 300 MHz): δ = 6.15 (s, 1H, CONH), 6.58 (s, 1H, =NNH, D_2O exchangeable), 7.45–7.55 (d, 4H, Ar C–H), 8.23 (s, 1H, C–H), 8.25–8.28 (d, 2H, benzothiazole C–H), 9.19 ppm (s, 1H, benzothiazole C–H); ^{13}C NMR ([D$_6$]DMSO, 300 MHz): δ = 117.76 (C7), 120.11 (C5), 122.34 (C4), 125.36 (C′4), 125.46 (C7a), 131.34 (C′2, C′6), 131.89 (C′3, C′5), 133.06 (C′1), 144.01 (C=N), 145.83 (C6), 155.10 (C3a), 157.42 (C=O), 174.17 ppm (C2); FAB: *m/z* 420.04 $[M+1]^+$; Anal. for $C_{15}H_{10}BrN_5O_3S$: calcd: C 42.87, H 2.40, N 16.67, found: C 42.89, H 2.43, N 16.64.

1-(4-Hydroxybenzylidene)-4-(6-nitrobenzothiazol-2-yl)semicarbazide (13): Yellow solid; mp: 239 °C; IR (KBr): $\tilde{\nu}$ = 3743.96 (O–H str), 3514.42 (N–H str), 3097.78 (aromatic C–H str), 1647.26 (C=O str), 1600.97 (C=C str), 1594.88 (C=N str), 1529.60, 1327.07 (Ar–NO_2 str), 1294.28 cm^{-1} (C–N str); ^{1}H NMR ([D$_6$]DMSO, D_2O exchange, 300 MHz): δ = 5.12 (s, 1H, O–H), 6.10 (s, 1H, CONH), 7.34 (s, 1H, =NNH, D_2O exchangeable), 6.83–7.55 (d, 4H, Ar C–H), 8.24 (s, 1H, C–H), 8.36–8.39 (d, 2H, benzothiazole C–H), 9.12 ppm (s, 1H, benzothiazole C–H); ^{13}C NMR ([D$_6$]DMSO, 300 MHz): δ = 116.95 (C′3, C′5), 117.74 (C7), 119.34 (C5), 122.02 (C4), 126.13 (C7a), 126.74 (C′1), 130.56 (C′2, C′6), 142.68 (C=N), 146.81 (C6), 155.41 (C3a), 158.62

(C=O), 160.81 (C′4), 173.81 ppm (C2); FAB: *m/z* 357.16 $[M+1]^+$; Anal. for $C_{15}H_{11}N_5O_4S$: calcd: C 50.42, H 3.10, N 19.60, found: C 50.45, H 3.08, N 19.57.

1-(4-Nitrobenzylidene)-4-(6-nitrobenzothiazol-2-yl)semicarbazide (14): Yellow solid; mp: 231 °C; IR (KBr): $\tilde{\nu}=3527.92$ (N–H str), 3095.85 (aromatic C–H str), 1647.26 (C=O str), 1596.88 (C=C str), 1570.11 (C=N str), 1525.74, 1327.07 (Ar–NO_2 str), 1296.21 cm^{-1} (C–N str); ^1H NMR ([D_6]DMSO, D_2O exchange, 300 MHz): $\delta=6.09$ (s, 1H, CONH), 6.46 (s, 1H, =NNH, D_2O exchangeable), 7.95–8.68 (d, 4H, Ar C–H), 8.11 (s, 1H, C–H), 8.41–8.48 (d, 2H, benzothiazole C–H), 9.16 ppm (s, 1H, benzothiazole C–H); ^{13}C NMR ([D_6]DMSO, 300 MHz): $\delta=117.65$ (C7), 120.91 (C5), 121.1 (C′3, C′5), 123.04 (C4), 125.43 (C7a), 130.31 (C′2, C′6), 140.05 (C′1), 144.17 (C=N), 145.86 (C6), 150.74 (C′4), 155.06 (C3a), 157.03 (C=O), 174.12 ppm (C2); FAB: *m/z* 386.18 $[M+1]^+$; Anal. for $C_{15}H_{10}N_6O_5S$: calcd: C 46.63, H 2.61, N 21.75, found: C 46.61, H 2.64, N 21.73.

1-(4-Methoxybenzylidene)-4-(6-nitrobenzothiazol-2-yl)semicarbazide (15): Yellow solid; mp: 257 °C; IR (KBr): $\tilde{\nu}=3460.41$ (N–H str), 3068.85 (aromatic C–H str), 2733.22 (alkane C–H), 1654.98 (C=O str), 1593.95 (C=C str), 1570.11 (C=N str), 1533.46, 1332.86 (Ar–NO_2 str), 1294.28 (C–N str), 1122.61 cm^{-1} (C–O str); ^1H NMR ([D_6]DMSO, D_2O exchange, 300 MHz): $\delta=3.76$ (s, 3H, OCH_3), 6.23 (s, 1H, CONH), 6.28 (s, 1H, =NNH, D_2O exchangeable), 6.87–7.63 (d, 4H, Ar C–H), 8.20 (s, 1H, C–H), 8.41–8.46 (d, 2H, benzothiazole C–H), 9.06 ppm (s, 1H, benzothiazole C–H); ^{13}C NMR ([D_6]DMSO, 300 MHz): $\delta=55.93$ (C″1, OCH_3), 114.35 (C′3, C′5), 117.81 (C7), 120.21 (C5), 122.46 (C4), 125.43 (C7a), 125.95 (C′1), 130.54 (C′2, C′6), 143.09 (C=N), 145.48 (C6), 155.32 (C3a), 157.33 (C=O), 163.25 (C′4), 174.56 ppm (C2); FAB: *m/z* 371.28 $[M+1]^+$; Anal. for $C_{16}H_{13}N_5O_4S$: calcd: C 51.75, H 3.53, N 18.86, found: C 51.72, H 3.55, N 18.89.

1-(4-(Dimethylamino)benzylidene)-4-(6-nitrobenzothiazol-2-yl)-semicarbazide (16): Yellow solid; mp: 207 °C; IR (KBr): $\tilde{\nu}=3458.48$ (N–H str), 3061.13 (aromatic C–H), 2943.47 (alkane C–H), 1570.11 (C=N str), 1654.98 (C=O str), 1533.46, 1329.00 (Ar–NO_2 str), 1300.07 cm^{-1} (C–N str); ^1H NMR ([D_6]DMSO, D_2O exchange, 300 MHz): $\delta=2.98$ (s, 6H, CH_3), 6.09 (s, 1H, CONH), 6.53–7.34 (d, 4H, Ar C–H), 7.17 (s, 1H, =NNH, D_2O exchangeable), 8.16 (s, 1H, C–H), 8.33–8.42 (d, 2H, benzothiazole C–H), 8.97 ppm (s, 1H, benzothiazole C–H); ^{13}C NMR ([D_6]DMSO, 300 MHz): $\delta=40.35$ (C‴1, C‴′1, CH_3), 113.98 (C′3, C′5), 117.46 (C7), 119.75 (C5), 121.99 (C4), 123.43 (C′1), 125.49 (C7a), 129.92 (C′2, C′6), 143.94 (C=N), 145.79 (C6), 152.08 (C′4), 155.17 (C3a), 156.89 (C=O), 174.56 ppm (C2); FAB: *m/z* 384.07 $[M+1]^+$; Anal. for $C_{17}H_{16}N_6O_3S$: calcd: C 53.12, H 4.20, N 21.86, found: C 53.09, H 4.22, N 21.89.

1-(2,3-Dichlorobenzylidene)-4-(6-nitrobenzothiazol-2-yl)semicarbazide (17): Yellow solid; mp: 254 °C; IR (KBr): $\tilde{\nu}=3460.41$ (N–H str), 3066.92 (aromatic C–H str), 1654.98 (C=O str), 1591.02 (C=C str), 1570.11 (C=N str), 1531.53, 1325.14 (Ar–NO_2 str), 1288.49 (C–N str), 752.26 cm^{-1} (C–Cl str); ^1H NMR ([D_6]DMSO, D_2O exchange, 300 MHz): $\delta=6.03$ (s, 1H, CONH), 6.66 (s, 1H, =NNH, D_2O exchangeable), 7.14–7.49 (m, 3H, Ar C–H), 8.17 (s, 1H, C–H), 8.51–8.56 (d, 2H, benzothiazole C–H), 8.99 ppm (s, 1H, benzothiazole C–H); ^{13}C NMR ([D_6]DMSO, 300 MHz): $\delta=117.36$ (C7), 120.32 (C5), 122.94 (C4), 125.58 (C7a), 127.93 (C′5), 128.67 (C′6), 130.86 (C′2), 132.86 (C′4), 133.59 (C′3), 134.42 (C′1), 143.25 (C=N), 145.82 (C6), 155.24 (C3a), 157.34 (C=O), 174.53 ppm (C2); FAB: *m/z* 409.36 $[M+1]^+$; Anal. for $C_{15}H_9Cl_2N_5O_3S$: calcd: C 43.92, H 2.21, N 17.07, found: C 43.95, H 2.20, N 17.04.

1-(2,6-Dichlorobenzylidene)-4-(6-nitrobenzothiazol-2-yl)semicarbazide (18): Yellow solid; mp: 236 °C; IR (KBr): $\tilde{\nu}=3460.41$ (N–H str), 3066.92 (aromatic C–H str), 1653.05 (C=O str), 1591.05 (C=C str), 1570.11 (C=N str), 1535.74, 1325.14 (Ar–NO_2 str), 1290.42 (C–N str), 752.26 cm^{-1} (C–Cl str); ^1H NMR ([D_6]DMSO, D_2O exchange, 300 MHz): $\delta=6.10$ (s, 1H, CONH), 6.19 (s, 1H, =NNH, D_2O exchangeable), 7.26–7.29 (m, 3H, Ar C–H), 8.15 (s, 1H, C–H), 8.59–8.61 (d, 2H, benzothiazole C–H), 9.18 ppm (s, 1H, benzothiazole C–H); ^{13}C NMR ([D_6]DMSO, 300 MHz): $\delta=117.54$ (C7), 120.02 (C5), 122.41 (C4), 125.83 (C7a), 127.19 (C′3, C′5), 132.01 (C′1), 134.08 (C′4), 135.62 (C′2, C′6), 143.55 (C=N), 145.98 (C6), 155.12 (C3a), 157.07 (C=O), 174.59 ppm (C2); FAB: *m/z* 409.39 $[M+1]^+$; Anal. for $C_{15}H_9Cl_2N_5O_3S$: calcd: C 43.92, H 2.21, N 17.07, found: C 43.89, H 2.23, N 17.05.

1-(2,4-Dichlorobenzylidene)-4-(6-nitrobenzothiazol-2-yl)semicarbazide (19): Yellow solid; mp: 242 °C; IR (KBr): $\tilde{\nu}=3462.34$ (N–H str), 3082.35 (aromatic C–H str), 1653.05 (C=O str), 1592.95 (C=C str), 1570.11 (C=N str), 1535.39, 1329.00 (Ar–NO_2 str), 1301.99 (C–N str), 750.33 cm^{-1} (C–Cl str); ^1H NMR ([D_6]DMSO, D_2O exchange, 300 MHz): $\delta=6.07$ (s, 1H, CONH), 6.49 (s, 1H, =NNH, D_2O exchangeable), 7.23–7.69 (m, 3H, Ar C–H), 8.13 (s, 1H, C–H), 8.57–8.64 (d, 2H, benzothiazole C–H), 9.08 ppm (s, 1H, benzothiazole C–H); ^{13}C NMR ([D_6]DMSO, 300 MHz): $\delta=117.58$ (C7), 120.28 (C5), 122.46 (C4), 125.80 (C7a), 126.99 (C′5), 130.48 (C′3), 131.43 (C′1), 132.56 (C′6), 135.65 (C′2), 137.98 (C′4), 142.95 (C=N), 145.85 (C6), 155.09 (C3a), 156.87 (C=O), 174.33 ppm (C2); FAB: *m/z* 409.45 $[M+1]^+$; Anal. for $C_{15}H_9Cl_2N_5O_3S$: calcd: C 43.92, H 2.21, N 17.07, found: C 43.91, H 2.24, N 17.04.

1-(3,4-Dimethoxybenzylidene)-4-(6-nitrobenzothiazol-2-yl)semicarbazide (20): Yellow solid; mp: 240 °C; IR (KBr): 3460.41 (N–H str), 3057.27 (aromatic C–H), 2947.33 (alkane C–H), 1654.98 (C=O str), 1568.18 (C=N str), 1533.46, 1329.00 (Ar–NO_2 str), 1301.99 (C–N str), 1292.35 cm^{-1} (C–O str); ^1H NMR ([D_6]DMSO, D_2O exchange, 300 MHz): $\delta=3.79$ (s, 6H, OCH_3), 6.25 (s, 1H, CONH), 7.38 (s, 1H, =NNH, D_2O exchangeable), 6.69–7.24 (dd, 3H, Ar C–H), 8.15 (s, 1H, C–H), 8.41–8.44 (d, 2H, benzothiazole C–H), 9.01 ppm (s, 1H, benzothiazole C–H); ^{13}C NMR ([D_6]DMSO, 300 MHz): $\delta=56.28$ (C″1, C‴′1, OCH_3), 114.38 (C′2), 115.33 (C′5), 117.92 (C7), 119.91 (C5), 122.13 (C4), 122.53 (C′6), 125.41 (C7a), 127.39 (C′1), 143.18 (C=N), 145.83 (C6), 149.83 (C′3), 152.18 (C′4), 155.21 (C3a), 157.16 (C=O), 173.93 ppm (C2); FAB: *m/z* 401.15 $[M+1]^+$; Anal. for $C_{17}H_{15}N_5O_5S$: calcd: C 50.87, H 3.77, N 17.45, found: C 50.89, H 3.74, N 17.48.

1-(2,5-Dimethoxybenzylidene)-4-(6-nitrobenzothiazol-2-yl)semicarbazide (21): Yellow solid; mp: 238 °C; IR (KBr): $\tilde{\nu}=3510.56$ ((N–H str), 3099.71 (aromatic C–H str), 1653.05 (C=O str), 1591.02 (C=C str), 1570.11 (C=N str), 1527.67, 1327.07 (Ar–NO_2 str), 1298.14 (C–N str), 1124.54 cm^{-1} (C–O str); ^1H NMR ([D_6]DMSO, D_2O exchange, 300 MHz): $\delta=3.78$ (s, 6H, OCH_3), 5.99 (s, 1H, CONH), 7.03 (s, 1H, =NNH, D_2O exchangeable), 6.75–7.13 (m, 3H, Ar C–H), 8.14 (s, 1H, C–H), 8.35–8.69 (d, 2H, benzothiazole C–H), 9.13 ppm (s, 1H, benzothiazole C–H); ^{13}C NMR ([D_6]DMSO, 300 MHz): $\delta=55.96$ (C″1, C‴′1, OCH_3), 114.38 (C′6), 115.32 (C′3), 117.48 (C′4), 117.88 (C7), 118.21 (C′1), 120.16 (C5), 122.19 (C4), 125.42 (C7a), 143.62 (C=N), 145.92 (C6), 152.93 (C′2), 153.81 (C′5), 155.18 (C3a), 157.14 (C=O), 174.37 ppm (C2); FAB: *m/z* 401.38 $[M+1]^+$; Anal. for $C_{17}H_{15}N_5O_5S$: calcd: C 50.87, H 3.77, N 17.45, found: C 50.84, H 3.78, N 17.48.

1-(3,4,5-Trimethoxybenzylidene)-4-(6-nitrobenzothiazol-2-yl)semicarbazide (22): Yellow solid; mp: 247 °C; IR (KBr): $\tilde{\nu}=3527.92$ (N–H str), 3093.92 (aromatic C–H str), 1647.26 (C=O str), 1594.88 (C=C str), 1570.11 (C=N str), 1525.74, 1327.07 (Ar–NO_2 str), 1296.21 (C–N str), 1124.54 cm^{-1} (C–O str); ^1H NMR ([D_6]DMSO, D_2O exchange, 300 MHz): $\delta=3.78$ (s, 9H, OCH_3), 6.14 (s, 1H, CONH), 6.24 (s, 1H, =NNH, D_2O exchangeable), 6.65 (s, 2H, Ar C–H), 8.16 (s, 1H, C–H), 8.47–8.50 (d, 2H, benzothiazole C–H), 8.98 ppm (s, 1H, ben-

zothiazole C–H); ^{13}C NMR ([D$_6$]DMSO, 300 MHz): δ = 55.91 (C″3, C″5, OCH_3), 56.29 (C″4, OCH_3), 108.19 (C′2, C′6), 117.23 (C7), 120.13 (C5), 122.39 (C4), 125.47 (C7a), 126.21 (C′1), 140.97 (C′4), 143.01 (C=N), 145.64 (C6), 150.95 (C′3, C′5), 155.03 (C3a), 157.23 (C=O), 174.75 ppm (C2); FAB: *m/z* 431.40 $[M+1]^+$; Anal. for $C_{18}H_{17}N_5O_6S$: calcd: C 50.11, H 3.97, N 16.23, found: C 50.08, H 3.94, N 16.26.

4-(6-Nitrobenzothiazol-2-yl)-1-(1-phenylethylidene)semicarbazide (23): Yellow solid; mp: 202 °C; IR (KBr): $\tilde{\nu}$ = 3460.41 (N–H str), 3064.99 (aromatic C–H str), 1654.98 (C=O str), 1568.18 (C=N str), 1531.53, 1329.00 (Ar–NO_2 str), 1292.35 cm^{-1} (C–N str); ^{1}H NMR ([D$_6$]DMSO, D$_2$O exchange, 300 MHz): δ = 0.81 (s, 6H, CH_3), 6.21 (s, 1H, CONH), 7.13 (s, 1H, =NNH, D$_2$O exchangeable), 7.45–7.73 (m, 5H, Ar C–H), 8.68–8.71 (d, 2H, benzothiazole C–H), 9.67 ppm (s, 1H, benzothiazole C–H); ^{13}C NMR ([D$_6$]DMSO, 300 MHz): δ = 20.01 (C″1, CH_3), 117.34 (C7), 120.21 (C5), 122.02 (C4), 124.96 (C7a), 128.32 (C′3, C′5), 129.1 (C′2, C′6), 129.9 (C′4), 133.91 (C′1), 145.75 (C6), 154.93 (C3a), 156.79 (C=O), 167.98 (C=N), 174.80 ppm (C2); FAB: *m/z* 355.29 $[M+1]^+$; Anal. for $C_{16}H_{13}N_5O_3S$: calcd: C 54.08, H 3.69, N 19.71, found: C 54.10, H 3.68, N 19.73.

1-(1-(4-Bromophenyl)ethylidene)-4-(6-nitrobenzothiazol-2-yl)semicarbazide (24): Yellow solid; mp: 235 °C; IR (KBr): $\tilde{\nu}$ = 3406.40 (N–H str), 3095.85 (aromatic C–H str), 1654.98 (C=O str), 1587.17 (C=C str), 1572.04 (C=N str), 1529.60, 1334.78 (Ar–NO_2 str), 1288.49 (C–N str), 549.73 cm^{-1} (C–Br str); ^{1}H NMR ([D$_6$]DMSO, D$_2$O exchange, 300 MHz): δ = 0.89 (s, 3H, CH_3), 6.17 (s, 1H, CONH), 7.23 (s, 1H, =NNH, D$_2$O exchangeable), 7.59 (dd, 4H, Ar C–H), 8.24–8.29 (d, 2H, benzothiazole C–H), 8.90 ppm (s, 1H, benzothiazole C–H); ^{13}C NMR ([D$_6$]DMSO, 300 MHz): δ = 19.11 (C″1, CH_3), 117.79 (C7), 120.18 (C5), 122.31 (C4), 125.42 (C′4), 125.56 (C7a), 131.39 (C′2, C′6), 131.85 (C′3, C′5), 133.24 (C′1), 145.90 (C6), 155.74 (C3a), 157.26 (C=O), 168.83 (C=N), 173.98 ppm (C2); FAB: *m/z* 433.95 $[M+1]^+$; Anal. for $C_{16}H_{12}BrN_5O_3S$: calcd: C 44.25, H 2.79, N 16.13, found: C 44.28, H 2.77, N 16.11.

1-(1-(4-Fluorophenyl)ethylidene)-4-(6-nitrobenzothiazol-2-yl)semicarbazide (25): Yellow solid; mp: 241 °C; IR (KBr): $\tilde{\nu}$ = 3458.48 (N–H str), 3095.85 (aromatic C–H str), 1654.98 (C=O str), 1592.95 (C=C str), 1570.11 (C=N str), 1531.53, 1327.07 (Ar–NO_2 str), 1290.42 cm^{-1} (C–N str); ^{1}H NMR ([D$_6$]DMSO, D$_2$O exchange, 300 MHz): δ = 0.94 (s, 3H, CH_3), 6.21 (s, 1H, CONH), 7.29 (s, 1H, =NNH, D$_2$O exchangeable), 7.04–7.93 (dd, 4H, Ar C–H), 8.35–8.69 (d, 2H, benzothiazole C–H), 9.13 ppm (s, 1H, benzothiazole C–H); ^{13}C NMR ([D$_6$]DMSO, 300 MHz): δ = 19.23 (C″1, CH_3), 114.52 (C′3, C′5), 117.81 (C7), 120.28 (C5), 122.13 (C4), 125.31 (C7a), 129.63 (C′1), 130.49 (C′2, C′6), 145.73 (C6), 155.67 (C3a), 156.87 (C=O), 165.19 (C′4), 168.74 (C=N), 173.85 ppm (C2); FAB: *m/z* 373.17 $[M+1]^+$; Anal. for $C_{16}H_{12}FN_5O_3S$: calcd: C 51.47, H 3.24, N 18.76, found: C 51.50, H 3.22, N 18.73.

1-(1-(4-Hydroxyphenyl)ethylidene)-4-(6-nitrobenzothiazol-2-yl)-semicarbazide (26): Yellow solid; mp: 176 °C; IR (KBr): $\tilde{\nu}$ = 3510.56 (O–H str), 3392.60 (N–H str), 3093.92 (aromatic C–H str)1647.26 (C=O str), 1575.89 (C=N str), 1531.53, 1329.00 (Ar–NO_2 str), 1294.28 cm^{-1} (C–N str); ^{1}H NMR ([D$_6$]DMSO, D$_2$O exchange, 300 MHz): δ = 0.86 (s, 6H, CH_3), 5.25 (s, 1H, Ar O–H), 6.14 (s, 1H, CONH), 7.22 (s, 1H, =NNH, D$_2$O exchangeable), 7.40–7.63 (m, 5H, Ar C–H), 8.54–8.59 (d, 2H, benzothiazole C–H), 9.35 ppm (s, 1H, benzothiazole C–H); ^{13}C NMR ([D$_6$]DMSO, 300 MHz): δ = 19.43 (C″1, CH_3), 116.5 (C′3, C′5), 117.46 (C7), 120.32 (C5), 122.41 (C4), 126.33 (C′1), 126.38 (C7a), 130.57 (C′2, C′6), 145.57 (C6), 155.11 (C3a), 157.24 (C=O), 161.02 (C′4), 168.76 (C=N), 173.96 ppm (C2); FAB: *m/z* 371.35 $[M+1]^+$; Anal. for $C_{16}H_{13}N_5O_4S$: calcd: C 51.75, H 3.53, N 18.86, found: C 51.78, H 3.55, N 18.89.

1-(Diphenylmethylene)-4-(6-nitrobenzothiazol-2-yl)semicarbazide (27): Yellow solid; mp: 190 °C; IR (KBr): $\tilde{\nu}$ = 3460.41 (N–H str), 3057.27 (aromatic C–H str), 1653.05 (C=O str), 1570.11 (C=N str), 1533.46, 1327.07 (Ar–NO_2 str), 1284.63 cm^{-1} (C–N str); ^{1}H NMR ([D$_6$]DMSO, D$_2$O exchange, 300 MHz): δ = 6.34 (s, 1H, CONH), 7.41 (s, 1H, =NNH, D$_2$O exchangeable), 7.59–8.01 (m, 10H, Ar C–H), 8.49–8.53 (d, 2H, benzothiazole C–H), 9.17 ppm (s, 1H, benzothiazole C–H); ^{13}C NMR ([D$_6$]DMSO, 300 MHz): δ = 117.89 (C7), 120.13 (C5), 122.72 (C4), 126.03 (C7a), 128.73(C′3, C′5, C″3, C″5), 129.32 (C′2, C′6, C″2, C″6), 131.27 (C′4, C″4), 133.11 (C′1, C″1), 146.07 (C6), 155.32 (C3a), 155.76 (C=N), 157.53 (C=O), 173.99 ppm (C2); FAB: *m/z* 417.39 $[M+1]^+$; Anal. for $C_{21}H_{15}N_5O_3S$: calcd: C 60.42, H 3.62, N 16.78, found: C 60.40, H 3.65, N 16.75.

1-((4-Chlorophenyl)(phenyl)methylene)-4-(6-nitrobenzothiazol-2-yl)semicarbazide (28): Yellow solid; mp: 245 °C; IR (KBr): $\tilde{\nu}$ = 3514.42 (N–H str), 3091.99 (aromatic C–H str), 1649.19 (C=O str), 1589.10 (C=C str), 1587.47 (C=N str), 1529.60, 1398.44 (Ar–NO_2 str), 1280.78 (C–N str), 692.47 cm^{-1} (C–Cl str); ^{1}H NMR ([D$_6$]DMSO, D$_2$O exchange, 300 MHz): δ = 6.37 (s, 1H, CONH), 7.28 (s, 1H, =NNH, D$_2$O exchangeable), 7.43–7.95 (m, 9H, Ar C–H), 8.53–8.57 (d, 2H, benzothiazole C–H), 9.32 ppm (s, 1H, benzothiazole C–H); ^{13}C NMR ([D$_6$]DMSO, 300 MHz): δ = 117.73 (C7), 120.45 (C5), 122.69 (C4), 125.64 (C7a), 128.97 (C″3, C″5), 128.99 (C′3, C′5), 129.32 (C″2, C″6), 130.59 (C′2, C′6), 130.97 (C′1), 131.21 (C″4), 132.94 (C″1), 136.58 (C′4), 145.68 (C6), 155.13 (C3a), 155.64 (C=N), 157.37 (C=O), 174.85 ppm (C2); FAB: *m/z* 451.76 $[M+1]^+$; Anal. for $C_{21}H_{14}ClN_5O_3S$: calcd: C 55.82, H 3.12, N 15.50, found: C 55.80, H 3.15, N 15.48.

1-((4-Hydroxyphenyl)(phenyl)methylene)-4-(6-nitrobenzothiazol-2-yl)semicarbazide (29): Yellow solid; mp: 208 °C; IR (KBr): $\tilde{\nu}$ = 3512.49 (O–H str), 3336.98 (N–H str), 3090.07 (aromatic C–H str), 1645.33 (C=O str), 1566.25 (C=N str), 1529.60, 1329.00 (Ar–NO_2 str), 1294.28 cm^{-1} (C–N str); ^{1}H NMR ([D$_6$]DMSO, D$_2$O exchange, 300 MHz): δ = 4.99 (s, 1H, Ar O–H), 6.09 (s, 1H, CONH), 7.23 (s, 1H, =NNH, D$_2$O exchangeable), 6.99–7.86 (m, 9H, Ar C–H), 8.28–8.39 (d, 2H, benzothiazole C–H), 8.98 ppm (s, 1H, benzothiazole C–H); ^{13}C NMR ([D$_6$]DMSO, 300 MHz): δ = 116.11 (C′3, C′5), 117.81 (C7), 120.72 (C5), 122.63 (C4), 125.43 (C′1), 126.61 (C7a), 128.33 (C″3, C″5), 129.12 (C″2, C″6), 130.58 (C′2, C′6), 131.21 (C″4), 132.11 (C″1), 146.23 (C6), 155.28 (C=N), 155.38 (C3a), 157.25 (C=O), 160.74 (C′4), 160.77 (C′4), 174.59 ppm (C2); FAB: *m/z* 433.41 $[M+1]^+$; Anal. for $C_{21}H_{15}N_5O_4S$: calcd: C 58.19, H 3.49, N 16.16, found: C 58.17, H 3.51, N 16.19.

1-(Bis(4-chlorophenyl)methylene)-4-(6-nitrobenzothiazol-2-yl)semicarbazide (30): Yellow solid; mp: 214 °C; IR (KBr): $\tilde{\nu}$ = 3514.42 (N–H str), 3093.92 (aromatic C–H), 1647.26 (C=O), 1566.25(C=N str), 1529.60, 1329.00 (Ar–NO_2 str), 1294.28 (C–N str), 750.33 cm^{-1} (C–Cl str); ^{1}H NMR ([D$_6$]DMSO, D$_2$O exchange, 300 MHz): δ = 6.32 (s, 1H, CONH), 7.26 (s, 1H, =NNH, D$_2$O exchangeable), 7.29–7.67 (m, 8H, Ar C–H), 8.36–8.42 (d, 2H, benzothiazole C–H), 9.22 ppm (s, 1H, benzothiazole C–H); ^{13}C NMR ([D$_6$]DMSO, 300 MHz): δ = 117.85 (C7), 120.16 (C5), 122.77 (C4), 126.01 (C7a), 128.94 (C′3, C′5, C″3, C″5), 130.54 (C′2, C′6, C″2, C″6), 131.18 (C′1, C″1), 136.76 (C′4, C″4), 146.14 (C6), 155.17 (C3a), 155.66 (C=N), 157.05 (C=O), 174.49 ppm (C2); FAB: *m/z* 485.93 $[M+1]^+$; Anal. for $C_{21}H_{13}Cl_2N_5O_3S$: calcd: C 51.86, H 2.69, N 14.40, found: C 51.89, H 2.68, N 14.43.

General procedure for the conventional synthesis of compounds 31–34

To a solution of 1-(6-nitrobenzothiazol-2-yl)semicarbazide **9** (0.003 mol) in EtOH, was added an equimolar quantity (0.003 mol)

of the appropriate 5-substituted isatin. The reaction mixture was adjusted to pH 5–6 by adding glacial acetic acid and held at reflux for 10–30 h. The contents of the flask were then poured into cold H_2O (30–60 mL), and the amorphous precipitate formed was filtered, dried, and recrystallized from 95% EtOH to produce the final products **31**–**34**.

4-(6-Nitrobenzothiazol-2-yl)-1-(2-oxoindolin-3-ylidene)semicarbazide (31): Yellow solid; mp: 209 °C; IR (KBr): $\tilde{\nu}$ = 3460.41 (N–H str), 3059.20 (aromatic C–H), 1747.57, 1653.05 (C=O str), 1570.11 (C=N str), 1533.46, 1329.00 (Ar–NO_2 str), 1290.42 cm^{-1} (C–N str); ^{1}H NMR ([D_6]DMSO, D_2O exchange, 300 MHz): δ = 6.18 (s, 1H, CONH), 7.27 (s, 1H, =NNH, D_2O exchangeable), 7.05–7.79 (m, 4H, oxindole C–H), 8.04 (s, 1H, N–H), 8.51–8.56 (d, 2H, benzothiazole C–H), 9.19 ppm (s, 1H, benzothiazole C–H); ^{13}C NMR ([D_6]DMSO, 300 MHz): δ = 117.76 (C′3a), 117.83 (C7), 120.16 (C5), 121.59 (C′7), 122.32 (C4), 124.31 (C′5), 125.43 (C7a), 129.23 (C′4), 130.99 (C′6), 132.86 (C′3), 133.67 (C=N), 145.75 (C6), 146.87 (C′7a), 155.30 (C3a), 157.05 (C=O), 167.48 (C′2), 174.53 ppm (C2); FAB: *m/z* 382.14 [*M*+1]$^+$; Anal. for $C_{16}H_{10}N_6O_4S$: calcd: C 50.26, H 2.64, N 21.98, found: C 50.23, H 2.67, N 21.96.

1-(5-Bromo-2-oxoindolin-3-ylidene)-4-(6-nitrobenzothiazol-2-yl)-semicarbazide (32): Red solid; mp: 178 °C; IR (KBr): $\tilde{\nu}$ = 3408.33 (N–H str), 3095.85 (aromatic C–H str), 1747.57, 1710.92 (C=O str), 1612.54 (C=C str), 1570.11 (C=N str), 1527.67, 1329.35 (Ar–NO_2 str), 1292.35 (C–N str), 462.93 cm^{-1} (C–Br str); ^{1}H NMR ([D_6]DMSO, D_2O exchange, 300 MHz): δ = 6.21 (s, 1H, CONH), 7.09 (s, 1H, =NNH, D_2O exchangeable), 7.45–7.88 (m, 3H, oxindole C–H), 8.12 (s, 1H, N–H), 8.49–8.53 (d, 2H, benzothiazole C–H), 9.06 ppm (s, 1H, benzothiazole C–H); ^{13}C NMR ([D_6]DMSO, 300 MHz): δ = 117.92 (C7), 118.44 (C′5), 120.07 (C′3a), 120.15 (C5), 122.53 (C4), 123.94 (C′7), 125.46 (C7a), 132.83 (C′3), 132.85 (C=N), 132.87 (C′4), 134.19 (C′6), 145.69 (C′7a), 145.79 (C6), 155.14 (C3a), 157.28 (C=O), 167.58 (C′2), 174.32 ppm (C2); FAB: *m/z* 460.19 [*M*+1]$^+$; Anal. for $C_{16}H_9BrN_6O_4S$: calcd: C 41.66, H 1.97, N 18.22, found: C 41.68, H 1.94, N 18.19.

1-(5-Chloro-2-oxoindolin-3-ylidene)-4-(6-nitrobenzothiazol-2-yl)-semicarbazide (33): Brown solid; mp: 248 °C; IR (KBr): $\tilde{\nu}$ = 3516.35 (N–H str), 3093.92 (aromatic C–H), 1741.78, 1647.26 (C=O str), 1570.11(C=N str), 1529.60, 1329.00 (Ar–NO_2 str), 1298.14 (C–N str), 1494.88 (C=C str), 750.33 cm^{-1} (C–Cl str); ^{1}H NMR ([D_6]DMSO, D_2O exchange, 300 MHz): δ = 6.13 (s, 1H, CONH), 7.41 (s, 1H, =NNH, D_2O exchangeable), 7.43–7.68 (m, 3H, oxindole C–H), 8.08 (s, 1H, N–H), 8.46–8.59 (d, 2H, benzothiazole C–H), 9.11 ppm (s, 1H, benzothiazole C–H); ^{13}C NMR ([D_6]DMSO, 300 MHz): δ = 117.89 (C7), 119.21 (C′3a), 120.18 (C5), 122.34 (C4), 122.91 (C′7), 125.39 (C7a), 129.51 (C′4), 129.98 (C′5), 131.31 (C′6), 132.75 (C′3), 132.83 (C=N), 144.93 (C′7a), 145.97 (C6), 155.24 (C3a), 157.03 (C=O), 167.52 (C′2), 174.48 ppm (C2); FAB: *m/z* 416.75 [*M*+1]$^+$; Anal. for $C_{16}H_9ClN_6O_4S$: calcd: C 46.11, H 2.18, N 20.16, found: C 46.13, H 2.20, N 20.15.

1-(5-Nitro-2-oxoindolin-3-ylidene)-4-(6-nitrobenzothiazol-2-yl)semicarbazide (34): Brown solid; mp: 212 °C; IR (KBr): $\tilde{\nu}$ = 3527.92 (N–H str), 3097.78 (aromatic C–H str), 1651.12, 1622.19 (C=O str), 1614.88 (C=C str), 1572.04 (C=N str), 1531.53, 1330.93 (Ar–NO_2 str), 1300.07 cm^{-1} (C–N str); ^{1}H NMR ([D_6]DMSO, D_2O exchange, 300 MHz): δ = 6.05 (s, 1H, CONH), 7.11 (s, 1H, =NNH, D_2O exchangeable), 7.98–8.64 (m, 3H, oxindole C–H), 8.23 (s, 1H, N–H), 8.48–8.52 (d, 2H, benzothiazole C–H), 9.26 ppm (s, 1H, benzothiazole C–H); ^{13}C NMR ([D_6]DMSO, 300 MHz): δ = 117.84 (C7), 118.76 (C′3a), 120.04 (C5), 122.37 (C4), 122.56 (C′7), 123.48 (C′6), 124.83 (C′4), 125.45 (C7a), 132.73 (C=N), 132.77 (C′3), 144.32 (C′5), 145.56 (C6), 153.12 (C′7a), 155.13 (C3a), 157.26 (C=O), 167.49 (C′2), 174.57 ppm (C2); FAB: *m/z* 427.26 [*M*+1]$^+$; Anal. for $C_{16}H_9N_7O_6S$: calcd: C 44.97, H 2.12, N 22.94, found: C 44.95, H 2.16, N 22.93.

In vitro MAO-B inhibition studies

Permission for animal studies was obtained from the Central Animal Ethical Committee of the University, Institute of Medical Sciences, Banaras Hindu University. Albino Wistar rats weighing between 200–220 g were obtained from Central Animal House, Institute of Medical Sciences, Banaras Hindu University (Registration No. 542/AB/CPCSEA).

Rat brain mitochondria were used as a source of the MAO-B isoform. Determination of IC_{50} values for the inhibition of MAO-B as well as the preparation of rat brain mitochondrial MAO-B were carried out under all suitable laboratory conditions. The final compounds **10**–**34** were evaluated for their in vitro MAO-B inhibitory activity according to the procedure reported by Tabor et al.[44] with necessary modifications using benzylamine as a substrate. Optimum conditions for the measurement of enzyme activity and IC_{50} values were sought in the experiment. The rat mitochondrial protein content was determined according to Lowry et al.[45] with bovine albumin as the standard. The test compounds **10**–**34** were dissolved in DMSO and added to the buffered incubation mixture such that the final DMSO concentration was 4%, which caused no MAO inhibition. Selegiline, safinamide, and isatin were taken as reference compounds for the determination of MAO-B activity. IC_{50} values were calculated at 95% confidence limits by using Prism GraphPad Software (version 5.0) from plots of inhibition percentages (calculated in relation to a sample of the enzyme treated under the same conditions without inhibitors) versus the logarithm of the inhibitor concentration.

Isolation of rat brain mitochondria[46]

All operations were carried out at 4 °C. Male and female adult Wistar rats weighing 200–220 g were decapitated. All brains were rapidly removed and homogenized with a Potter–Elvehjem homogenizer in cold 0.32 M sucrose and 50 mM Tris·HCl, pH 8.2 (10:1, *v/w*). The homogenate was centrifuged twice at 1000 *g* for 5 min at 4 °C. The resulting supernatant was centrifuged at 20000 *g* for 20 min. The mitochondrial pellet obtained was suspended in 100 mM sodium phosphate buffer, pH 7.4 (4:1, *v/w*), fractionated in plastic vials to 500 μL samples, and stored at −80 °C. Before use, mitochondria were diluted with 100 mM sodium phosphate buffer to give a working solution of 0.84 (mg protein) mL^{-1}.

MAO-B inhibitory activity assay[47]

An aliquot was made to contain a mixture of 55 μL mitochondrial suspension [0.84 (mg protein) mL^{-1}], 90 μL 50 mM Tris·HCl buffer pH 8.2, and 30 μL solubilizing solution (control or inhibitor solution at five different concentrations). The reaction was started by adding 25 μL benzylamine (0.1 M, substrate for MAO-B) for the determination of MAO-B activity. The mixture was incubated at 37 °C for 30 min, and the reaction was stopped by the addition of 1 mL of 3% ice-cold $ZnSO_4$ solution. It was subsequently mixed by vortexing for 10 s and then centrifuged at 3000 rpm for 15 min. The supernatant was taken up, and the absorbance was taken at λ 250 nm (formation of benzaldehyde) for MAO-B estimation. All the assays were performed in duplicate, and were repeated twice. Control experiments were carried out without inhibitor, and blanks were run without mitochondrial suspension.

Computational studies

In an attempt to obtain insight into the affinity and possible binding modes of 6-nitrobenzothiazole-derived semicarbazones **10**–**34** within the active site of MAO-B, molecular docking experiments were performed. All computational studies were carried out on PC-based machines running Windows 7 (x86) as operating system. The MarvinSketch 5.6 module of Chemaxon tools was obtained http://www.chemaxon.com. Python 2.7: language was obtained from http://www.python.com, Cygwin C:\program and Python 2.5 were simultaneously obtained from http://www.cygwin.com. Molecular Graphics Laboratory (MGL) tools 1.5.4 and AutoDock 4.2 were obtained from http://www.scripps.edu. Discovery Studio Visualizer 3.1 and PyMOL 1.3 were obtained from http://www.accelrys.com and http://www.pymol.org, respectively.

Protein preparation

The X-ray crystallographic structure of human recombinant MAO-B was obtained from the PDB (http://www.rcsb.org). The structure of MAO-B co-crystallized (in complex) with safinamide (PDB ID: 2V5Z, resolution: 1.6 Å)[48] was selected as receptor model. This model was selected due to the relatively high resolution of the crystallographic structure and also on the basis of observation that in the complex between MAO-B and safinamide, the side chain of Ile 199 is rotated out of the normal conformation, thus allowing fusion of the entrance and substrate cavities. This is the preferred conformation when the relatively large inhibitors, which span both the entrance and substrate cavities, bind to the active site of MAO-B.

Coordinate file preparation

Computational studies were carried out on only one subunit of the MAO-B enzyme. The PDB file of MAO-B was edited, and the α-chain was removed together with the complexed inhibitor (safinamide). All the water molecules and all non-interacting ions were also removed. This refinement in the crystal structure of MAO-B was carried out with the help of Discovery Studio Visualizer. An extended PDB format, termed as a PDBQT file, was used for coordinate files which includes atomic partial charges. AutoDock Tools was used for creating PDBQT files from traditional PDB files.[49]

Docking methodology

Lamarckian genetic algorithm (LGA)[50] for ligand conformational searching, which is a hybrid of a genetic algorithm and a local search algorithm, was employed in this study. This algorithm first builds a population of individuals (genes), each being a different random conformation of the docked molecule. Each individual is then mutated to acquire a slightly different translation and rotation, and the local search algorithm then performs energy minimizations on a user-specified proportion of the population of individuals. The individuals with low resulting energy are transferred to the next generation, and the process is then repeated. The algorithm is called Lamarckian because every new generation of individuals is allowed to inherit the local search adaptations of their parents.

The test ligands **10**–**34** and standard ligand (safinamide) were built using MarvinSketch module of Chemaxon tools and optimized using "Prepare Ligands" in AutoDock 4.2 for docking studies. The optimized ligand molecules in PDBQT format were docked into the refined MAO-B model using AutoDock 4.2.[50]

The refined protein molecule (PDB ID: 2V5Z) was initially subjected to addition of all hydrogen atoms to the macromolecule, which is a step necessary for correct calculation of partial atomic charges followed by the calculation of Gasteiger charges for each atom of the macromolecule in AutoDock 4.2. The grid maps were calculated using AutoGrid (version 4.2), one of the utility programs of AutoDock. In all docking, a grid of size $50\times50\times50$ points in *x*, *y*, and *z* directions was built, then the maps were centered on the N5 atom of the flavin (FAD) in the catalytic site of the protein. A grid spacing of 0.375 Å (approximately one fourth of the length of a carbon–carbon covalent bond) and a distance-dependent function of the dielectric constant were used for the calculation of the energetic map. Additionally, an electrostatic map and a desolvation map were also calculated.[51] Rapid energy evaluation was achieved by pre-calculating atomic affinity potentials for each atom in the ligand molecule. In the AutoGrid procedure, the MAO-B receptor was embedded on a three-dimensional grid point,[52] and the energy of interaction for each atom in the ligand was encountered. The grid maps were calculated by AutoGrid, one for each atom type present in the ligand being docked. Thus, the grid parameter file (receptor.gpf) was generated and saved. This is followed by the generation of docking parameter file (ligand.dpf). This helps to make the docking calculations fast.

The various important docking parameters selected for LGA includes population size of 150 individuals, 2.5 million energy evaluations, maximum of 27000 generations, maximum number of top individuals to automatically survive to next generation of 1, gene mutation rate of 0.02, crossover rate of 0.8, 10 docking runs and random initial positions and conformations. The probability of performing local search on an individual in the population was set to 0.06.

AutoDock was run several times to get various docked conformations, and used to analyze the predicted docking energy. The binding sites for these molecules were selected based on the ligand binding pocket of the templates. AutoDock tools provide various methods to analyze the results of docking simulations, such as conformational similarity, visualizing the binding site and its energy, and other parameters like intermolecular energy and inhibition constant. For each ligand, ten best poses were generated and scored using AutoDock 4.2 scoring functions.[53] At the end of docking, ligands with the most favorable free energy of binding were selected as the resultant complex structure. The same above procedure was repeated separately for all the ligands.

To determine the accuracy of this docking protocol, the reference inhibitor safinamide was docked into the active site of MAO-B, and the resulting binding pose was compared with that of co-crystallized safinamide. This procedure was repeated three times, and the best ranked solutions of safinamide exhibited an RMSD value of 1.80 Å from the position of the co-crystallized safinamide (Figure 3a). Because RMSD values <2.0 Å generally indicate that the docking protocol is capable of accurately predicting the binding orientation of the ligand,[54] this protocol was deemed suitable for the docking of inhibitors into the MAO-B active site. The docking solutions were ranked according to their respective dock score values.

Acknowledgements

The authors thank Dr. Sairam K., Department of Pharmaceutics, Indian Institute of Technology (BHU), Varanasi for his assistance in MAO-B screening. R.K.P.T. is thankful to the University Grants

Commission, New Delhi (India) for the award of Junior Research Fellowship.

Keywords: benzothiazoles · drug design · MAO-B inhibitors · molecular docking · semicarbazones

[1] M. Reyes-Parada, A. Fierro, A. P. Iturriaga-Vasquez, B. K. Cassels, *Curr. Enzyme Inhib.* **2005**, *1*, 85 – 95.
[2] P. H. Yu, in *Neuromethods V* (Eds.: A. A. Boulton, G. B. Baker, P. H. Yu), *Neurotransmitter Enzymes*, Humana, Clifton, **1986**, pp. 235 – 272.
[3] M. D. Berry, A. V. Juorio, I. A. Paterson, *Prog. Neurobiol.* **1994**, *42*, 375 – 391.
[4] J. P. Johnston, *Biochem. Pharmacol.* **1968**, *17*, 1285 – 1297.
[5] J. Bertoni, L. Elmer, in *The Role of MAO-B Inhibitors in the Treatment of Parkinson's Disease* (Eds.: M. Ebadi, R. F. Pfeiffer), CRC, Boca Raton, **2005**, pp. 691 – 704.
[6] D. E. Edmondson, C. Binda, J. Wang, A. K. Upadhyay, A. Mattevi, *Biochemistry* **2009**, *48*, 4220 – 4230.
[7] A. E. Lang, A. Lees, *Mov. Disord.* **2002**, *17*, 38 – 44.
[8] W. Weyler, Y. P. Hsu, X. O. Breakefield, *Pharmacol. Ther.* **1990**, *47*, 391 – 417.
[9] M. B. H. Youdim, D. Edmondson, K. F. Tipton, *Nat. Rev. Neurosci.* **2006**, *7*, 295 – 309.
[10] A. M. Cesura, A. Pletscher, *Prog. Drug Res.* **1992**, *38*, 171 – 297.
[11] P. Pacher, E. Kohegyi, V. Keckemeti, S. Furst, *Curr. Med. Chem.* **2001**, *8*, 89 – 100.
[12] P. Pacher, V. Keckemeti, *Curr. Med. Chem.* **2004**, *11*, 925 – 943.
[13] T. A. Ban, *J. Neural Transm.* **2001**, *108*, 707 – 716.
[14] B. Blackwell, *Drugs* **1981**, *21*, 201 – 219.
[15] M. Yamada, H. Yasuhara, *Neurotoxicology* **2004**, *25*, 11 – 20.
[16] M. V. Rudorfer, V. Z. Potter, *Drugs* **1989**, *37*, 713 – 738.
[17] S. Palhagen, E. Heinonen, J. Hagglund, T. Kaugesaar, O. Maki-Ikola, R. Palm, *Neurology* **2006**, *66*, 1200 – 1206.
[18] D. R. Guay, *Am. J. Geriatr. Pharmacother.* **2006**, *4*, 330 – 346.
[19] P. Riederer, W. Danielczyk, E. Grunblatt, *Neurotoxicology* **2004**, *25*, 271 – 277.
[20] M. B. H. Youdim, M. Fridkin, H. Zheng, *J. Neural Transm.* **2004**, *111*, 1455 – 1471.
[21] M. C. Carreiras, J. L. Marco, *Curr. Pharm. Des.* **2004**, *10*, 3167 – 3175.
[22] S. Y. Son, J. Ma, Y. Kondou, M. Yoshimura, E. Yamashita, T. Tsukihara, *Proc. Natl. Acad. Sci. USA* **2008**, *105*, 5739 – 5744.
[23] F. Hubalek, C. Binda, A. Khalil, M. Li, A. Mattevi, N. Castagnoli, D. E. Edmondson, *J. Biol. Chem.* **2005**, *280*, 15761 – 15766.
[24] a) L. De Colibus, M. Li, C. Binda, A. Lustig, D. E. Edmondson, A. Mattevi, *Proc. Natl. Acad. Sci. USA* **2005**, *102*, 12684 – 12689; b) C. Binda, P. Newton-Vinson, F. Hubalek, D. E. Edmondson, A. Mattevi, *Nat. Struct. Biol.* **2002**, *9*, 22 – 26; c) C. Binda, F. Hubalek, M. Li, Y. Herzig, J. Sterling, D. E. Edmondson, A. Mattevi, *J. Med. Chem.* **2004**, *47*, 1767 – 1774; d) C. Binda, M. Li, F. Hubalek, N. Restelli, D. E. Edmondson, A. Mattevi, *Proc. Natl. Acad. Sci. USA* **2003**, *100*, 9750 – 9755; e) C. Binda, F. Hubalek, M. Li, D. E. Edmondson, A. Mattevi, *FEBS Lett.* **2004**, *564*, 225 – 228.
[25] K. F. Tipton, M. D. Houslay, N. J. Garrett, *Nat. New Biol.* **1973**, *246*, 213 – 214.
[26] P. H. Yu, in *Monoamine Oxidase: Structure, Function and Altered Functions* (Eds.: T. P. Singer, R. W. von Korff, D. L. Murphy), Academic Press, San Diego, **1979**, pp. 233 – 244.
[27] F. Mazouz, S. Gueddari, C. Burstein, D. Mansuy, R. Milcent, *J. Med. Chem.* **1993**, *36*, 1157 – 1167.
[28] F. Mazouz, L. Lebreton, R. Milcent, C. Burstein, *Eur. J. Med. Chem.* **1990**, *25*, 659 – 671.
[29] J. Wouters, F. Moureau, G. Evrard, J. Koenig, S. Jegham, P. George, F. Durant, *Bioorg. Med. Chem.* **1999**, *7*, 1683 – 1693.
[30] K. F. Tipton, *Biochem. J.* **1972**, *128*, 913 – 919.
[31] A. Dar, K. M. Khan, H. S. Ateeq, S. Khan, S. Rahat, S. Perveen, C. T. Supuran, *J. Enzyme Inhib. Med. Chem.* **2005**, *20*, 269 – 274.
[32] A. Binda, J. Wang, M. Li, F. Hubalek, A. Mattevi, D. E. Edmondson, *Biochemistry* **2008**, *47*, 5616 – 5625.
[33] a) F. Chimenti, E. Maccioni, D. Secci, A. Bolasco, P. Chimenti, A. Granese, O. Befani, P. Turini, S. Alcaro, F. Ortuso, M. C. Cardia, S. Distinto, *J. Med. Chem.* **2007**, *50*, 707 – 712; b) F. Chimenti, E. Maccioni, D. Secci, A. Bolasco, P. Chimenti, A. Granese, S. Carradori, S. Alcaro, F. Ortuso, M. Yanez, F. Orallo, R. Cirilli, R. Ferretti, F. La Torre, *J. Med. Chem.* **2008**, *51*, 4874 – 4880.
[34] S. Bernard, C. Paillat, T. Oddos, M. Seman, R. Milcent, *Eur. J. Med. Chem.* **1995**, *30*, 471 – 482.
[35] a) F. Chimenti, D. Secci, A. Bolasco, P. Chimenti, A. Granese, S. Carradori, E. Maccioni, M. C. Cardia, M. Yanez, F. Orallo, S. Alcaro, F. Ortuso, R. Cirilli, R. Ferretti, S. Distinto, J. Kirchmair, T. Langer, *Bioorg. Med. Chem.* **2010**, *18*, 5063 – 5070; b) F. Chimenti, A. Bolasco, D. Secci, P. Chimenti, A. Granese, S. Carradori, M. Yanez, F. Orallo, F. Ortuso, S. Alcaro, *Bioorg. Med. Chem.* **2010**, *18*, 5715 – 5723.
[36] G. Bora-Tatar, D. Dayangaç-Erden, A. S. Demir, S. Dalkara, K. Yelekçi, H. Erdem-Yurter, *Bioorg. Med. Chem.* **2009**, *17*, 5219 – 5228.
[37] N. E. Vergel, J. L. Lopez, F. Orallo, D. Vina, D. M. Buitrago, E. del Olmo, J. A. Mico, M. F. Guerrero, *Life Sci.* **2010**, *86*, 819 – 824.
[38] a) L. H. A. Prins, J. P. Petzer, S. F. Malan, *Eur. J. Med. Chem.* **2010**, *45*, 4458 – 4466; b) K. Boppana, P. K. Dubey, S. A. R. P. Jagarlapudi, S. Vadivelan, G. Rambabu, *Eur. J. Med. Chem.* **2009**, *44*, 3584 – 3590.
[39] W. J. Geldenhuys, A. S. Darvesh, M. O. Funk, C. J. Van der Schyf, R. T. Carroll, *Bioorg. Med. Chem. Lett.* **2010**, *20*, 5295 – 5298.
[40] F. Ooms, R. Frederick, F. Durant, J. P. Petzer, N. Castagnoli, C. J. Van der Schyf, J. Wouters, *Bioorg. Med. Chem. Lett.* **2003**, *13*, 69 – 73.
[41] a) S. N. Pandeya, A. S. Raja, J. P. Stables, *J. Pharm. Pharm. Sci.* **2002**, *5*, 266 – 271; b) A. S. Raja, S. N. Pandeya, S. S. Panda, J. P. Stables, *Pharm. Chem. J.* **2007**, *41*, 302 – 307.
[42] N. Siddiqui, A. Rana, S. A. Khan, M. A. Bhat, S. E. Haque, *Bioorg. Med. Chem. Lett.* **2007**, *17*, 4178 – 4182.
[43] a) V. Glover, J. M. Halket, P. J. Watkins, *J. Neurochem.* **1988**, *51*, 656 – 659; b) A. E. Medvedev, B. Goodwin, A. Clow, J. Halket, V. Glover, M. Sandler, *Biochem. Pharmacol.* **1992**, *44*, 590 – 592.
[44] C. W. Tabor, H. Tabor, S. M. Rosenthal, *J. Biol. Chem.* **1954**, *208*, 645 – 661.
[45] O. H. Lowry, N. J. Rosebrough, A. L. Forr, R. T. Randall, *J. Biol. Chem.* **1951**, *193*, 265 – 275.
[46] P. H. Reinhart, W. M. Taylor, F. L. Bygrave, *Biochem. J.* **1982**, *204*, 731 – 735.
[47] H. Park, M. U. Choi, *Korean Biochem. J.* **1983**, *16*, 189 – 198.
[48] a) C. Caccia, R. Maj, M. Calabresi, S. Maestroni, L. Faravelli, L. Curatolo, P. Salvati, R. G. Fariello, *Neurology* **2006**, *67*, S18 – 23; b) C. Binda, J. Wang, L. Pisani, C. Caccia, A. Carotti, P. Salvati, D. E. Edmondson, A. Mattevi, *J. Med. Chem.* **2007**, *50*, 5848 – 5852.
[49] A. Madeswaran, M. Umamaheswari, K. Asokkumar, T. Sivashanmugam, V. Subhadradevi, P. Jagannath, *J. Comput. Method Mol. Des.* **2011**, *1*, 65 – 72.
[50] D. S. Goodsell, G. M. Morris, A. J. Olson, *J. Mol. Recognit.* **1996**, *9*, 1 – 5.
[51] J. Konc, J. T. Konc, M. Penca, D. Janezic, *Acta Chim. Slov.* **2011**, *58*, 396 – 401.
[52] M. Umamaheswari, A. Madeswaran, K. Asokkumar, T. Sivashanmugam, V. Subhadradevi, P. Jagannath, *Bangladesh J. Pharmacol.* **2011**, *6*, 117 – 123.
[53] A. Madeswaran, M. Umamaheswari, K. Asokkumar, T. Sivashanmugam, V. Subhadradevi, P. Jagannath, *Orient. Pharm. Exp. Med.* **2012**, *12*, 157 – 161.
[54] J. Boström, J. R. Greenwood, J. Gottfries, *J. Mol. Graph. Model.* **2003**, *21*, 449 – 462.

Received: October 22, 2012
Revised: December 19, 2012
Published online on January 16, 2013